

# Indexing Metric Spaces for Exact Similarity Search

LU CHEN, Aalborg University, Denmark  
YUNJUN GAO, Zhejiang University, China  
XUAN SONG, Zhejiang University, China  
ZHENG LI, Zhejiang University, China  
XIAOYE MIAO, Zhejiang University, China  
CHRISTIAN S. JENSEN, Aalborg University, Denmark

---

With the continued digitalization of societal processes, we are seeing an explosion in available data. This is referred to as big data. In a research setting, three aspects of the data are often viewed as the main sources of challenges when attempting to enable value creation from big data: volume, velocity and variety. Many studies address volume or velocity, while much fewer studies concern the variety. Metric space is ideal for addressing variety because it can accommodate any type of data as long as its associated distance notion satisfies the triangle inequality. To accelerate search in metric space, a collection of indexing techniques for metric data have been proposed. However, existing surveys each offers only a narrow coverage, and no comprehensive empirical study of those techniques exists. We offer a survey of all the existing metric indexes that can support exact similarity search, by i) summarizing all the existing partitioning, pruning and validation techniques used for metric indexes, ii) providing the time and storage complexity analysis on the index construction, and iii) report on a comprehensive empirical comparison of their similarity query processing performance. Here, empirical comparisons are used to evaluate the index performance during search as it is hard to see the complexity analysis differences on the similarity query processing and the query performance depends on the pruning and validation abilities related to the data distribution. This article aims at revealing different strengths and weaknesses of different indexing techniques in order to offer guidance on selecting an appropriate indexing technique for a given setting, and directing the future research for metric indexes.

CCS Concepts: • **General and reference** → **Surveys and overviews**; • **Information Systems** → **Data Management Systems**; • **Theory of Computation** → **Design and Analysis of Algorithms**

Additional Key Words and Phrases: Metric spaces, Indexing and Querying, Metric Similarity Search

## ACM Reference Format:

Lu Chen, Yunjun Gao, Xuan Song, Zheng Li, Xiaoye Miao, and Christian S. Jensen. 2020. Indexing Metric Spaces for Exact Similarity Search. *ACM Comput. Surv.* XX, X, Article XXX (May 2020), 39 pages. <https://doi.org/124564>.

---

## 1 INTRODUCTION

Massive and increasing volumes of data are being generated. For example, as shown in Fig. 1, massive spatio-temporal data is being generated by moving cars, sensors, GIS and so on; millions

---

This work was supported in part by the National Key Research and Development Program of China under Grant No. 2018YFB1004003, the 973 Program of China under Grant No. 2015CB352502, the NSFC under Grants No. 61972338, 61902343, and 61522208, the NSFC-Zhejiang Joint Fund under Grant No. U1609217, and the DiCyPS project.

Author's addresses: Lu Chen and Christian S. Jensen, Department of Computer Science, Aalborg University, Aalborg, Denmark, email: {luchen, csj}@cs.aau.dk; Yunjun Gao (corresponding author), Xuan Song, and Zheng Li, College of Computer Science, Zhejiang University, China, email: {gaoyj, xsong, lzheng}@zju.edu.cn; Xiaoye Miao, Center for Data Science, Zhejiang University, China, email: miaoxy@zju.edu.cn.

Permission to make digital or hard copies of part or all of this work for personal or classroom use is granted without fee provided that copies are not made or distributed for profit or commercial advantage and that copies bear this notice and the full citation on the first page. Copyrights for third-party components of this work must be honored. For all other uses, contact the owner/author(s).

© 20XX Copyright held by the owner/author(s). 0730-0301...\$15.00  
<https://doi.org/124564>

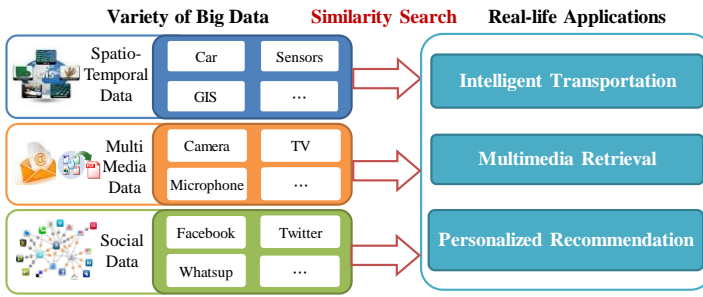


Fig. 1 Applications of Similarity Search on Variety of Big Data

of multimedia data is being generated from cameras, microphones, TVs, and so on; while billions of social data is being generated from social media including Facebook, Twitter, Whatsup and so on. This represents an opportunity to create value from data, benefitting businesses as well as society as a whole. On the flipside, it also presents difficult challenges due to the sheer volume, velocity and variety of the data. Volume refers to the characteristic that the amount of data is massive. Next, velocity refers to the facts that the data arrives at a rapid rate. Finally, variety captures the property that the data comes from a wide range of sources and is diverse in terms of its structure and data types. Many studies address volume or velocity, while much fewer studies concern the variety. Metric space is ideal for addressing variety because it can accommodate any type of data as long as its associated similarity/distance notion satisfies the triangle inequality. Hence, by utilizing metric space, unified solutions can be developed for processing the diverse big data.

Due to the general notation of a metric space, search in metric space plays an important role in a wide range of real-life applications, with similarity search being a prominent type of search. Given a query object, similarity search finds its similar objects according to a definition of similarity. In intelligent transportation, similarity queries can be used to find the nearest restaurant for a user. In multimedia retrieval, similarity queries can be utilized to identify images similar to a specified image. In recommender systems, similarity queries can be employed to generate personalized recommendations for users. In addition, similarity queries can be used to accelerate data mining tasks, e.g., similarity search can be used as the first step of clustering or outlier detection. In all the above applications, metric space can be used to model the wealth of data types (e.g., locations, images, and strings), and can be used to support a wide range of distance metrics used for comparing the similarity of objects, including the shortest path distance for locations, the  $L_p$ -norm and SIFT for images, and the edit distance for strings. Metric space requires no assumptions on the representations of objects and any similarity notation satisfying the triangle inequality can be accommodated.

A number of indexing techniques exist that aim to accelerate search in metric spaces. The main goal of this work is to present a complete survey that can describe and analyze all the metric indexes. Although several works [32, 60, 99, 124] survey metric indexing techniques, they fail to provide comprehensive theoretical and experimental analysis. This work is an extension of our previously work [37] that provides an empire study on pivot-based metric indexing. As an extension, we include following fresh contributions in this paper: (i) we have focused on all the metric indexes that can support exact similarity search; (ii) we have added a summary of all the partitioning methods and provided more complete pruning filtering and validation techniques used for all the metric indexes; (iii) we have included the time and storage complexity analysis on the index construction; and (iv) we have conducted empirical comparisons on the exact metric similarity search performance based on all metric indexes.

The rest of the paper is organized as follows. Section 2 presents the basic concepts of metric indexes. Section 3 summarizes the all the techniques used for metric indexes. Sections 4 and 5

Table 1. Symbols used Throughout the Paper

Symbols	Descriptions
$O, C, P$	The set of data, centers, and pivots
$S$	The sample set of $O$
$o, c, p$	The object, the center, and the pivot
$n, n_s$	The cardinality of dataset $O$ and the cardinality of the sample set $S$
$s$	The storage size of each object
$m$	the tree-arity or the capacity of a tree node
$l, l_c$	The number of pivots and the number of candidate pivots
$g$	The number of pivots in a pivot group
$x$	The cost of space-filling curve transformation
$d(o, p)$	The distance between objects $o$ and $p$
$n_d$	The number of values for discrete $d()$ or the maximum distance of continuous $d()$
$MRQ(q, r)$	The metric range query with the query object $q$ and the search radius $r$
$MkNNQ(q, k)$	The $k$ nearest neighbor query with the query object $q$ and the number $k$

describe two different types of metric indexes respectively. Experimental results and findings are reported in Section 6. Finally, Section 7 concludes the paper and provides future directions.

## 2 Basic Concepts

We provide the basic definitions of metric space and metric similarity search, and introduce all the categorized metric indexes. Table 1 summarizes the symbols used throughout the paper.

### 2.1 Metric Space

A metric space is a two-tuple  $(M, d)$ , in which  $M$  is an object domain and  $d$  is a distance function for measuring the “similarity” between objects in  $M$ . In particular, the distance function  $d$  has four properties:

- Symmetry:  $d(q, o) = d(o, q)$ ;
- Non-negativity:  $d(q, o) \geq 0$ ;
- Identity:  $d(q, o) = 0$  iff  $q = o$ ;
- Triangle inequality:  $d(q, o) \leq d(q, p) + d(p, o)$ .

According to the definition of metric spaces, they can support any type of data as long as the distance measurement satisfies the above four properties. Hence, metric space is a general space. A typical example of metric spaces is the vector space associated with the distance measurement  $L_p$ -norm ( $p \geq 1$ ). Another example of metric spaces is a set of strings, which uses the edit distance to measure the similarity. Note that, there exist various indexes designed for a particular metric space, e.g., R-tree [13], KD-tree [14], and TV-tree [71] for vector spaces, where properties (e.g., the dimension information of vector spaces) of this particular metric space can be utilized to accelerate the search. However, these specific properties are not available in general metric spaces, and thus, cannot be used to prune the search space in general metric spaces. In other words, the specific properties of vectors cannot be applied for the strings. By using metric space, a unified solution can be developed for processing all kinds of data. However, due to the generality of metric space, we can only use the four distance properties discussed above to prune the search space and thus accelerate the search. More specially, Section 3 will detail all the techniques that can be used in general metric spaces.

**Intrinsic dimensionality of metric space.** The dimensionality is an important feature of vector space data. The higher dimensionality the vector space is, the worse search performance will be. However, the general metric space is not limited to the vector space, it also includes other data types, such as strings and sets. Instead of dimensionality, we can use the intrinsic

dimensionality that is applied for any data type in metric space. As discussed in many previous studies [15, 32, 43, 75, 97, 105, 121, 124], the intrinsic dimensionality can be calculated as  $\mu^2/2\sigma^2$ , where  $\mu$  and  $\sigma^2$  are the mean and variance of the distances between data objects. Hence, the intrinsic dimensionality of metric space data is defined according to the data distribution. Same as vector space, the intrinsic dimensionality affect the metric search performance.

## 2.2 Metric Similarity Query

We define metric similarity search, including the metric range query and the metric  $k$  nearest neighbor query. We only focus on metric similarity query in this survey. This is because similarity query is an important and typical query type that can be used to verify the efficiency and effectiveness of the designed indexes.

*Definition 2.1. (METRIC RANGE QUERY).* Given an object set  $O$ , a query object  $q$ , and a search radius  $r$  in a metric space, a metric range query returns the objects in  $O$  that are within distance  $r$  of  $q$ , i.e.,  $MRQ(q, R) = \{o \in O \wedge d(q, o) \leq R\}$ .

*Definition 2.2. (METRIC  $k$  NEAREST NEIGHBOR QUERY).* Given an object set  $O$ , a query object  $q$ , and an integer  $k$  in a metric space, a metric  $k$  nearest neighbor query finds  $k$  objects in  $O$  that are most similar to  $q$ , i.e.,  $MkNNQ(q, k) = \{S \mid S \subseteq O \wedge |S| = k \wedge \forall s \in S, \forall o \in O - S, d(q, s) \leq d(q, o)\}$ .

Consider the DNA set  $O = \{\text{"ATAGCTCA"}, \text{"AATCTGA"}, \text{"AATCTGT"}, \text{"AAAACGG"}, \text{"CATCTGT"}\}$ , where edit distance is used to measure similarity between DNAs. An example of metric range query finds the DNAs from  $O$  with edit distances to the query DNA "CAATCTGT" no larger than 2, i.e.,  $MRQ(\text{"CAATCTGT"}, 2) = \{\text{"AATCTGA"}, \text{"AATCTGT"}, \text{"CATCTGT"}\}$ . An example of metric  $k$  nearest neighbor query finds 2 nearest DNAs from  $O$  to the query DNA "CAATCTGT", i.e.,  $MkNNQ(\text{"CAATCTGT"}, 2) = \{\text{"AATCTGT"}, \text{"CATCTGT"}\}$ .

**Strategies to answer  $MkNNQ$  using  $MRQ$ .** An  $MkNNQ$  can be answered by an  $MRQ$ , if the distance from  $q$  to its  $k^{\text{th}}$  nearest neighbor, denoted as  $ND_k$ , is known. However,  $ND_k$  is not known when a query is issued. Three typical methods exist for computing  $MkNNQ$  [19, 61].

- (i) **Strategy 1:** It utilizes  $MRQ$  with incremental search radius. Specifically, an  $MRQ$  with a small search radius is performed first, and then the search radius is increased gradually until  $k$  nearest neighbors are found. Although this strategy tries to avoid visiting objects already verified, it still needs to traverse the metric index multiple times, resulting in high query cost.
- (ii) **Strategy 2:** It sets the search radius to infinity and then verifies the objects in order, where the search radius is tighten using verification. As described in Sections 4 and 5,  $MkNNQ$  processing usually takes the second strategy due to better search performance.
- (iii) **Strategy 3:** It finds  $k$  the candidate NNs for the query object, and use the candidates to calculate the current farthest  $k$ -th NN distance. Then a  $MRQ$  is performed using the current farthest  $k$ -th NN distance as the search radius to refine the result. However, the performance of this strategy relies on the candidates found at the beginning.

**Performance Metrics for Metric Similarity Search.** The total time of a metric similarity query includes the CPU time and the IO time. In order to evaluate the performance of metric similarity search, we use running time (i.e., the response time) as the total time of a metric similarity query. The distance computation is usually costly (e.g., edit distance) in metric spaces. Thus, the distance computation cost is a dominate cost of CPU time, and we can use the number of distance computations to estimate the CPU time. Since external indexes are stored as pages on disk, the IO time can be estimated using the number of page accesses during the search. Note that, for metric indexes stored in the main memory, their IO time equals to 0. As a summary, in order to evaluate the performance of metric similarity search, three metrics are used, including (i) the running time, (ii) the number of distance computations, and (iii) the number of page accesses.

Table 2. Metric Indexes for Exact Similarity Search

Index	Category	Space Cost	Construction Cost
BST <sup>[69]</sup> , MBST <sup>[92]</sup>	CP-Index	$O(ns)$	$\Omega(n \log_2 n)$
VT <sup>[46][46]</sup>	CP-Index	$O(ns)$	$\Omega(n \log_3 n)$
BU-Tree <sup>[72]</sup>	CP-Index	$O(ns)$	$O(n^3)$
GHT <sup>[115]</sup>	CP-Index	$O(ns)$	$\Omega(n \log_2 n)$
GNAT <sup>[21]</sup> , EGNAT <sup>[76][89]</sup>	Hybrid	$O(ns + nm)$	$\Omega(nm \log_m n)$
SAT <sup>[29][84][85]</sup>	CP-Index	$O(ns)$	$O(n \log n / \log \log n)$
DSAT <sup>[86][87][88][90][91]</sup>	CP-Index	$O(ns)$	$O(mn \log_m n)$
DSACLT <sup>[12][22]</sup>	CP-Index	$O(ns)$	$O(mn \log_m^n / k)$
HRG <sup>[54]</sup> , $k$ NNG <sup>[96]</sup>	CP-Index	$O(ns)$	$O(n^2)$
M-tree <sup>[38][42][110]</sup>	CP-Index	$O(ns + ns/m)$	$O(mn \log_m n)$
PM-tree <sup>[112]</sup>	Hybrid	$O(n(s+l) + n(s+l)/m + ls)$	$O(n(m+l) \log_m n)$
LC <sup>[28][31]</sup> , DLC <sup>[91]</sup>	CP-Index	$O(ns)$	$O(n^2/m)$
HC <sup>[56][57]</sup>	CP-Index	$O(ns)$	$O(n \log_2^n / m)$
D-index <sup>[48][49][123]</sup>	Hybrid	$O(ns + nl + ls)$	$O(nl)$
MB <sup>+</sup> -Tree <sup>[63]</sup>	CP-Index	$O((n+n/m)(s+\log_2^n / m + \log_2 n d))$	$O(n \log_2^n / m + nm \log_m n)$
AESA <sup>[102][117]</sup> , ROAESA <sup>[118]</sup>	P-Index	$O(ns + n^2)$	$O(n^2)$
iAESA <sup>[51][52]</sup>	P-Index	$O(ns + n^2)$	$O(n^2 \log_2 n)$
LAESA <sup>[79]</sup>	P-Index	$O(ns + ls + nl)$	$O(nl)$
TLAESA <sup>[80][113]</sup>	Hybrid	$O(ns + ls + nl)$	$\Omega(n \log_2 n + nl)$
EPT <sup>[103]</sup>	P-Index	$O(ns + lgs + nl)$	$O(nlg)$
EPT <sup>*</sup> <sup>[37]</sup>	P-Index	$O(ns + lcs + nl)$	$O(nllcns)$
CPT <sup>[82]</sup>	P-Index	$O(ns + ns/m + ls + nl)$	$O(mn \log_m n + nl)$
BKT <sup>[23]</sup>	P-Index	$O(ns + lnd)$	$O(nl)$
FQT <sup>[10]</sup> , FHQT <sup>[11]</sup> , FQA <sup>[31]</sup>	P-Index	$O(ns + nl)$	$O(nl)$
VPT <sup>[114][115][122]</sup> , DVPT <sup>[58]</sup>	P-Index	$O(ns)$	$O(n \log_2 n)$
MVPT <sup>[18][19]</sup>	P-Index	$O(ns)$	$O(n \log_m n)$
Omni-family <sup>[20][66]</sup>	P-Index	$O(ns + nl + nl/m + ls)$	$O(nl + nm \log_m n)$
SPB-tree <sup>[33][34]</sup>	P-Index	$O(ns + n + n/m + ls)$	$O(nlx + nm \log_m n)$
M-index <sup>[93]</sup>	Hybrid	$O(ns + nl + n + n/m + ls)$	$\Omega(nl \log^n / m + nm \log_m n)$
M-index <sup>*</sup> <sup>[37]</sup>	Hybrid	$O(ns + nl + n + n/m + nl/m + ls)$	$\Omega(nl \log^n / m + nm \log_m n)$

### 2.3 Metric Indexes for Exact Metric Similarity Queries

In order to support efficient metric similarity queries, various metric indexes are proposed. Table 2 summarizes all metric indexes that can support exact metric similarity search. They can be classified into two board categories, i.e., compact-partitioning techniques (termed as CP-Index) and pivot-based techniques (termed as P-Index). In addition, hybrid indexes combine compact-partitioning and pivot-based methods (termed as Hybrid). In the table, we provide the space and time cost analysis of index construction. Some metric indexes (e.g., BST family, GHT family, TLAESA and M-index) are unbalanced trees, and thus, we assume that the tree structure is balanced to obtain the optimal (i.e., lower bound) construction cost  $\Omega(\cdot)$ . Here, metric similarity search complexity performed on each index is omitted, because it depends the pruning ability related to the data distribution. As stated in Section 2.2, we will use three performance metrics to demonstrate the metric similarity search performance via various experiments.

Compact-partitioning based methods divide the space as compact as possible and try to prune unqualified partitions during search. Bisector Tree (BST) [69] is a binary tree that uses a center with a covering radius to represent a partition. Many variants of BST including Monotonous BST (MBST) [92], Voronoi Tree (VT) [46, 47] and Bottom-Up Tree (BU-Tree) [72] are proposed to improve the efficiency of BST. Generalized Hyperplane Tree (GHT) [115] is similar as BST

without storing covering radius. Spatial Approximation Tree (SAT) [30, 84, 85] is based on Voronoi diagrams, which attempts to approximate the structure of a Delaunay graph. Dynamic and secondary memory extensions of SAT includes DSAT [86, 87, 88, 90, 91] and DSACLT [12, 22]. In addition, Hyperspherical Region Graph (HRG) [54] is in-memory index similar to DSACLT, and  $k$ -Nearest-Neighbor Graph ( $k$ NNG) [96] is a graph structure similar to SAT. Next, the M-tree [38, 42, 110] is a height-balanced tree that is optimized for secondary memory. It is the first dynamic MAM that can support data insertions and deletions. Several variants of M-trees, including MM-tree [98], Slim-tree [68, 111],  $M^+$ -tree [127],  $BM^+$ -tree [128] and CM-tree [7] that use different split functions to reduce the overlap among nodes,  $M^x$ -tree [65] and Onion-tree [26] that try to reduce the tree construction cost, DBM-tree [119, 120] that allows a controlled unbalance to better fit the dataset density variations, and Antipole Tree [26] that aims to minimize number of clusters. In addition, many variants BP-tree [1],  $M^*$ -tree [108], DF-tree [67], PM-tree [112], and  $PM^*$ -tree [108] combines multiple local or global pivots to further improve the pruning ability of M-tree. More recently, variants  $M^\#$ -tree and  $PM^\#$ -tree [100] are designed to avoid duplications of data. List of Clusters (LC) [28, 31] employs a list of clusters to trade construction time for query time, and its dynamic version is Dynamic LC (DLC) [91]. The construction efficiency of LC can be improved by constructing multiple layers (resulting in Hierarchy of Clusters HC [56, 57]) or by using cluster reduction [6]. Metric  $B^+$ -tree ( $MB^+$ -tree) [63] uses the relaxed generalized partitioning technique or ball partitioning technique to recursively partition the dataset and build the binary tree, while each leaf node denotes a cluster. In particular, each object can be represented as a fixed length bit string after partitioning and indexed by a  $B^+$ -tree.

Pivot-based methods store pre-computed distances from every object in the database to a set of pivots and then utilize these distances and the triangle inequality to prune unqualified objects during search. Approximating Eliminating Search Algorithm (AESA) [102, 117] uses a pivot table to preserve the distances from each object to other objects. To improve the search efficiency, Reduced-Overhead AESA (ROAESA) [118] and iAESA [51, 52] are designed while its data structure is same as AESA, where iAESA sorts the pre-computed distances for each object. To reduce the storage for AESA, Linear AESA (LAESA) [79] only keeps the distances from every object to selected pivots. Different from LAESA that uses a single set of pivots, Extreme Pivot Table  $EPT^{(*)}$  [37, 103] selects several sets of pivots. Clustered Pivot-table (CPT) [82] clusters the pre-computed distances to improve the query efficiency. Burkhard-Keller Tree (BKT) [23] is a tree structure designed for discrete distance functions. In contrast to BKT, where pivots at individual levels are different, Fixed Queries Tree (FQT) [10], Fixed Height FQT (FHQT) [11], and Fixed Queries Array (FQA) [31] use the same pivot for all nodes at the same level of the tree. Vantage-Point Tree (VPT) [114, 115, 122] is designed for continuous distance functions, and it has also been extended to a dynamic structure DVPT [58] and generalized to  $m$ -ary trees yielding MVPT [18, 19]. The Omni-family [20, 66] employs selected pivots together with existing structures (e.g., the R-tree) to index pre-computed distances. Space-filling curve and Pivot-based  $B^+$ -tree (SPB-tree) [33, 34] utilizes a space-filling curve to map pre-computed distances to integers, which are then indexed by the  $B^+$ -tree.

Hybrid methods that combine compact partitioning with the use of pivots have appeared. Generalized Near-Neighbor Access Tree (GNAT) [21] is an  $m$ -way generalization of GHT, which utilizes the generalized hyperplane partition method to partition the dataset and also uses cut-regions [73] defined by pivots to accelerate similarity search. In addition, a dynamic structure Evolutionary Geometric Near-neighbor Access Tree (EGNAT) has also been proposed [76, 89]. By combining the generalized partitioning and ball partitioning techniques, Tree LAESA (TLAESA) [80, 113] extends from LAESA and organizes the data as a tree. The D-index [48, 49, 123] combines the hash partitioning and the pivot mapping. It is a multilevel structure that hashes objects into buckets, which are search-separable. The PM-tree [112] also uses cut-regions defined by pivots to accelerate similarity queries on the M-tree. The M-Index $^{(*)}$  [37, 93] generalizes the

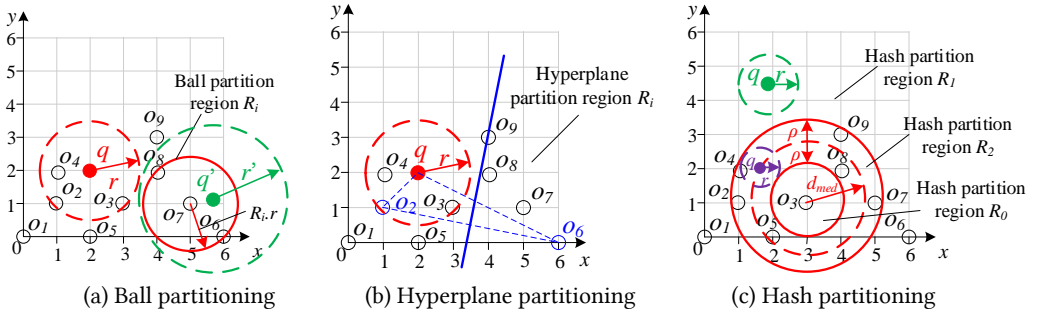


Fig. 1. Illustration of Partitioning Methods

iDistance [64] technique for general metric spaces, which compacts the objects by using pre-computed distances to their closest pivots.

## 2.4 Other Metric Indexes

This survey aims to summarize all the metric indexes that can support exact metric similarity search, and thus, metric indexes designed to support other metric queries are omitted. For example, to answer metric similarity joins, eD-index [50] extended from D-index is designed. To answer probabilistic range query, UP-Index [4] and UPB-tree/UPB-forest [35, 36] are proposed to index uncertain metric data. To support indexing multiple metric spaces,  $M^2$ -tree [39],  $M^3$ -tree [25], and Reference  $R^*/RR^*$ -tree [55] are proposed.

To further improve the metric similarity query efficiency, high quality approximate answers instead of exact results can be returned, resulting in approximate metric similarity search. To answer approximate metric similarity search, many metric indexes are developed, including approximate M-tree variants [40, 70, 109, 125, 126], hash based methods [8, 9, 78], permutation-based indexes [3, 29, 53, 81, 83, 116], and  $k$ NN graph based methods [74, 95, 106, 107], to name but a few. P-Sher tree [59] is built by using the sample of query objects. DAHC-tree [2] is optimized according to the global data distribution for high-dimension space.

In addition, metric indexes can further use other techniques (e.g., short term memories [101], bit operations [45], regrouping [104], parallel computing [20, 94] and cost-model-based distance distribution [41]) to improve the query efficiency. Different from individual metric index, an index framework that combines different metric indexes is also discussed in [77].

## 3 Techniques for Metric Indexing and Querying

We summarize all the partitioning methods for the compact-partitioning based metric indexes, and pivot-based filtering and validation for all the metric indexes.

### 3.1 Partitioning Methods

There exist three types of partitioning methods, i.e., ball partitioning, generalized hyperplane partitioning, and hash partitioning, as described below.

*Definition 3.1. (BALL PARTITIONING).* Given a center  $c$  and a radius  $r$ , then the set of objects  $o$  ( $\in O$ ) in the partition  $R_i$ , obtained via ball partitioning, is defined as  $\{o \mid o \in O \wedge d(o, c) \leq r\}$ .

Considering the example illustrated in Fig. 1(a), given a center  $o_7$  and a radius  $d(o_7, o_6)$ , then we can obtain the corresponding ball partition  $R_i = \{o_6, o_7, o_8\}$ . In order to solve the curse of high intrinsic dimensionality, the radius of ball partitioning can be set to  $2^d$ , where  $d$  denotes the intrinsic dimensionality of the dataset [16, 62]. This strategy can be applied to any metric index that uses ball partitioning technique to build the metric index for high intrinsic dimensionality.

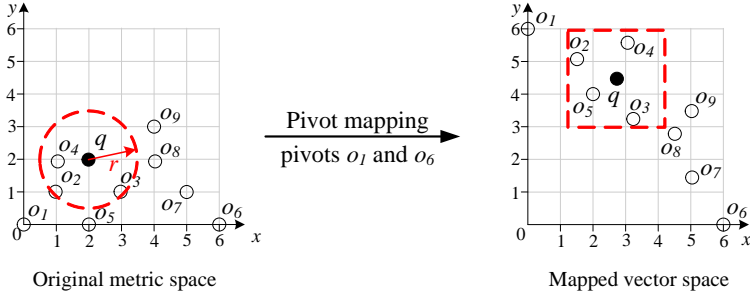


Fig. 2. Pivot Mapping

**Definition 3.2. (GENERALIZED HYPERPLANE PARTITIONING).** Given a set  $C$  of centers, let  $c_i$  be the center of a partition region  $R_i$ . The set of objects  $o$  ( $\in O$ ) in the partition  $R_i$ , obtained by generalized hyperplane partitioning, is defined as  $\{o \mid o \in O \wedge \forall c_j \neq c_i, d(o, c_i) \leq d(o, c_j)\}$ .

Considering the example illustrated in Fig. 1(b), given two centers  $o_2$  and  $o_6$ , we can get two hyperplane partition regions  $R_1 = \{o_1, o_2, o_3, o_4, o_5\}$  and  $R_2 = \{o_6, o_7, o_8, o_9\}$ . In addition, the generalized hyperplane partitioning can be relaxed by using an addition threshold  $\delta$  [44, 63], where the set of objects  $o$  ( $\in O$ ) in the partition  $R_i$ , obtained by relaxed generalized hyperplane partitioning, is defined as  $\{o \mid o \in O \wedge \forall c_j \neq c_i, d(o, c_i) \leq d(o, c_j) + \delta\}$ . This relaxed hyperplane partitioning method can be used in hyperplane partitioning based indexes (e.g., BST, GNAT).

**Definition 3.3. (HASH PARTITIONING).** Given a hash function  $h$ , the set of objects  $o$  ( $\in O$ ) in the partition  $R_i$ , obtained by the hash partitioning, is defined as  $\{o \mid o \in O \wedge h(o) = i\}$ .

For metric indexes, a particular hash function, i.e.,  $\rho$ -split function  $bps^\rho(c, o)$  uses a center  $c$  and the medium distance  $d_{med}$  to partition the data file into three subsets below. Note that, the median distance  $d_{med}$  is relative to  $c$  and it is defined so that the number of objects with distances smaller than  $d_{med}$  is the same as the number of objects with distances larger than  $d_{med}$ .

$$bps^\rho(c, o) = \begin{cases} 0 & \text{if } d(c, o) \leq d_{med} - \rho \\ 1 & \text{if } d(c, o) > d_{med} + \rho \\ - & \text{otherwise} \end{cases} \quad (1)$$

Here, “-” denotes the last partition, i.e., the exclusion partition. Considering an example illustrated in Fig. 1(c), given a center  $o_3$ , we can get three separated has partitions, i.e.,  $R_0 = \{o_3\}$ ,  $R_1 = \{o_1, o_6\}$  and  $R_2 = \{o_2, o_4, o_5, o_7, o_8, o_9\}$ . Note that,  $R_2$  is called as the exclusion partition. The  $\rho$ -split function can be generalized to a set of centers. Give a set of centers  $C$  whose cardinality is  $m$ , the object can be divided into  $2^m + 1$  partitions. Hence,  $bps^\rho(C, o) = bps^\rho(c_i, o) \times 2^{i-1}$  ( $c_i \in C, 1 \leq i \leq m$ ) if  $bps^\rho(c_i, o) = 0$  or  $1$ ; otherwise,  $bps^\rho(C, o) = 2^m$ .

### 3.2 Pivot mapping

Using well-chosen pivots, the objects in a metric space can be mapped to data points in a vector space. Given a pivot set  $P = \{p_1, p_2, \dots, p_l\}$ , a metric space  $(M, d)$  can be mapped to a vector space  $(R^l, L_\infty)$ . Specifically, an object  $q$  in the metric space is represented as a point  $\phi(q) = \langle d(q, p_1), d(q, p_2), \dots, d(q, p_l) \rangle$  in the vector space.

Consider the example in Fig. 2, where the  $L_2$ -norm is used as the distance function. If  $P = \{o_1, o_6\}$ , the object set in the original metric space can be mapped to the data points in a two-dimensional vector space, in which the  $x$ -axis denotes  $d(o_i, o_1)$  and the  $y$ -axis represents  $d(o_i, o_6)$  for any object  $o_i$ . As an example, object  $o_5$  is mapped to point  $\langle 2, 4 \rangle$ .

### 3.3 Pivot-based Filtering and Validating

Since the triangle inequality is the only property that can be used for reduce the search space for general metric spaces, we summarize seven filtering and validating lemmas below. Note that, for both compact-partitioning and pivot-based metric indexes, centers and pivots are combined with the triangle inequality for pruning and validation. In other words, a center used for compact partitioning methods can be regarded as a pivot of pivot-based methods. First, based on the pivot mapping, the pivot-based filtering [33] can be used to avoid unnecessary similarity computations.

**LEMMA 3.1 (PIVOT FILTERING).** *Given a set  $P = \{p_1, p_2, \dots, p_l\}$  of pivots, a query object  $q$ , and a search radius  $r$ , let  $SR(q)$  be a mapped search region such that  $SR(q) = \{[d(q, p_0) - r, d(q, p_0) + r], [d(q, p_1) - r, d(q, p_1) + r], \dots, [d(q, p_l) - r, d(q, p_l) + r]\}$ . If a mapped data  $\phi(o) = \langle d(o, p_1), d(o, p_2), \dots, d(o, p_l) \rangle$  locates outside  $SR(q)$ , then the original data  $o$  can be pruned safely.*

**PROOF.** Assume, to the contrary, that there exists an object  $o$  that satisfies  $d(q, o) \leq r$ , but  $\phi(o) \notin SR(q)$  (i.e.,  $\exists p_i \in P, d(o, p_i) > d(q, p_i) + r$  or  $d(o, p_i) < d(q, p_i) - r$ ). According to the triangle inequality,  $d(q, o) \geq |d(q, p_i) - d(o, p_i)| > r$ , which contradicts our assumption. The proof completes.  $\square$

Since the pre-computed distances  $\phi(o)$ s are stored together with object  $o$  in a metric index, we can avoid distance computations involving object  $o$  if  $\phi(o) \notin SR(q)$ , based on Lemma 3.1. Consider the example in Fig. 2 where the dotted rectangle represents the search region  $SR(q)$ . Here, object  $o_1$  can be pruned as  $\phi(o_1) \notin SR(q)$ . Also, Lemma 3.1 can be utilized to prune an entire region (i.e., a minimum bounding box that contains multiple  $\phi(o)$ s) if it does not intersect  $SR(q)$ . In the sequel, based on the ball partitioning, a range-pivot filtering technique [122] is developed below.

**LEMMA 3.2 (RANGE-PIVOT FILTERING).** *Given a ball partition region  $R_i$  with the center  $R_i.p$  and the radius  $R_i.r$ , a query object  $q$ , and a search radius  $r$ , if  $d(q, R_i.p) > R_i.r + r$ , then  $R_i$  can be pruned.*

**PROOF.** For any object  $o$  in  $R_i$ , if  $d(q, R_i.p) > R_i.r + r$ , then  $d(q, o) \geq d(q, R_i.p) - d(o, R_i.p) > R_i.r + r - d(o, R_i.p)$  due to the triangle inequality. As  $d(o, R_i.p) \leq R_i.r$  according to Definition 3.1, then we can derive that  $d(q, o) > r$ . Hence, any object  $o$  in  $R_i$  cannot be in the final result set, and  $R_i$  can be pruned safely, which completes the proof.  $\square$

Consider the example depicted in Fig. 1(a), where the red dotted line denotes the search region, and the red solid circle denotes the ball region  $R_i = \{o_6, o_7, o_8\}$  with its center  $R_i.p = o_7$  and its radius  $R_i.r = d(o_7, o_6)$ . As  $d(q, R_i.p) > R_i.r + r$ ,  $R_i$  can be pruned due to Lemma 3.2.

Note that, for an object  $o$  located inside the ball region  $R_i$ , if we record its distance  $d(o, R_i.p)$  to the partition center  $R_i.p$ , Lemma 3.2 can be applied to pruning this object by replacing  $R_i.r$  with  $d(o, R_i.p)$ . Hence, Lemma 3.2 can be also used for pruning single objects. Next, based on the generalized hyperplane partitioning, a double-pivot filtering technique [122] is developed below.

**LEMMA 3.3 (DOUBLE-PIVOT FILTERING).** *Given two pivots  $p_i$  and  $p_j$ , a query object  $q$ , and a search radius  $r$ , if  $d(q, p_i) - d(q, p_j) > 2 \times r$ , then  $R_i$  can be pruned safely, as  $p_i$  is the corresponding pivot for the partition region  $R_i$ .*

**PROOF.** For every  $o$  in  $R_i$ , according to the definition of  $R_i$ ,  $d(o, p_i) \leq d(o, p_j)$ . Based on the triangle inequality, we have  $d(q, p_i) \leq d(o, p_i) + d(q, o)$  and  $d(q, p_j) \geq d(o, p_j) - d(q, o)$ . Thus, we can derive that  $d(q, p_i) - d(q, p_j) \leq d(o, p_i) + d(q, o) - d(o, p_j) + d(o, q) \leq 2 \times d(q, o)$  as  $d(o, p_i) \leq d(o, p_j)$ . If  $d(q, p_i) - d(q, p_j) > 2 \times r$ , then  $d(q, o) > r$ . Therefore, no object  $o$  ( $o \in R_i$ ) can be a real answer object, and  $R_i$  can be pruned safely. The proof completes.  $\square$

Consider the example shown in Fig. 1(b), where  $o_2$  and  $o_6$  are two pivots. Since  $d(q, o_6) - d(q, o_2) > 2 \times r$ ,  $R_i = \{o_6, o_7, o_8, o_9\}$  can be discarded safely according to Lemma 3.3.

**LEMMA 3.4 (EXCLUSIVE FILTERING).** *Given a  $\rho$ -split function  $bps^\rho(c, o)$ , a query object  $q$ , and a search radius  $r$ , if  $r \leq \rho$  and  $bps^{\rho-r}(c, q) = \text{'-'}^*$ , then objects in partitions  $R_0$  and  $R_1$  can be pruned safely;*

if  $bps^{r-\rho}(c, q) = 0$ , then objects in partition  $R_1$  can be pruned safely; if  $bps^{r-\rho}(c, q) = 1$ , then objects in partition  $R_0$  can be pruned safely.

PROOF. If  $r \leq \rho$  and  $bps^{r-\rho}(c, q) = \text{'-'}'$ , then we can get that  $d_{med} - \rho + r < d(q, c) \leq d_{med} + \rho - r$ . For objects  $o$  in  $R_0$  (i.e.,  $d(c, o) \leq d_{med} - \rho$ ),  $d(q, o) \geq d(q, c) - d(c, o) > d_{med} - \rho + r - d_{med} + \rho = r$ , and thus objects in  $R_0$  can be pruned safely; For objects  $o$  in  $R_1$  (i.e.,  $d(c, o) > d_{med} + \rho$ ),  $d(q, o) \geq d(c, o) - d(c, q) > d_{med} + \rho - d_{med} - \rho + r = r$ , and thus objects in  $R_1$  can be pruned safely.

If  $bps^{r-\rho}(c, q) = 0$ , then we can get  $d(q, c) \leq d_{med} - r + \rho$ . For objects in  $R_1$  (i.e.,  $d(c, o) > d_{med} + \rho$ ),  $d(q, o) \geq d(c, o) - d(q, c) > d_{med} + \rho - d_{med} + r - \rho > r$ . Hence, objects in  $R_1$  can be pruned.  $\square$

If  $bps^{r-\rho}(c, q) = 1$ , then we can get  $d(q, c) > d_{med} + r - \rho$ . For objects  $o$  in  $R_0$  (i.e.,  $d(c, o) \leq d_{med} - \rho$ ),  $d(q, o) \geq d(q, c) - d(c, o) > d_{med} + r - \rho - d_{med} + \rho > r$ . Hence, objects in  $R_0$  can be pruned.  $\square$

Consider in the example shown in Fig. 1(c) and assume that the search region  $SR(q, r)$  is a purple dotted circle. The partitions  $R_0$  and  $R_1$  can be pruned safely due to  $r \leq \rho$  and  $bps^{r-\rho}(c, q) = \text{'-'}'$ . Here, in Lemma 3.4, we use one center for  $\rho$ -split function to illustrate the exclusive filtering. However, Lemma 3.4 can also be extended to multiple centers.

Lemmas 3.1 through 3.4 are pivot filtering techniques. Nonetheless, a distance computation is still needed for verifying each object that cannot be pruned. Hence, validation techniques can be proposed to save unnecessary verifications.

**LEMMA 3.5 (PIVOT VALIDATION).** Given a pivot set  $P$ , a query object  $q$ , and a search radius  $r$ , if there exists, for an object  $o$  in  $O$ , a pivot  $p_i (\in P)$  satisfying  $d(o, p_i) \leq r - d(q, p_i)$ , then  $o$  is validated to be an actual answer object.

PROOF. Given a query object  $q$ , an object  $o$ , and a pivot  $p_i$ ,  $d(q, o) \leq d(o, p_i) + d(q, p_i)$  because of the triangle inequality. If  $d(o, p_i) \leq r - d(q, p_i)$ , then  $d(q, o) \leq r - d(q, p_i) + d(q, p_i) = r$ . Thus,  $o$  is guaranteed to be contained in the search region, which completes the proof.  $\square$

Back to the example in Fig. 2(b), object  $o_2$  can be validated directly without computing the distance  $d(q, o_2)$  due to  $d(o_2, o_1) = r - d(q, o_1)$  according to Lemma 3.5.

**LEMMA 3.6 (RANGE-PIVOT VALIDATION).** Given a ball partition region  $R_i$  with the center  $R_i.p$  and the radius  $R_i.r$ , a query object  $q$ , and a search radius  $r$ , if  $d(q, R_i.p) \leq r - R_i.r$ , then objects in  $R_i$  should be validated to be actual answer objects.

PROOF. For any object  $o$  contained in  $R_i$  (i.e.,  $d(o, R_i.p) \leq R_i.r$ ), if  $d(q, R_i.p) \leq r - R_i.r$ , then  $d(q, o) \leq d(o, R_i.p) + d(q, R_i.p) \leq r - R_i.r + R_i.r = r$ . Hence,  $o$  is in the search region according to Definition 2.1, and all the objects in  $R_i$  should be validated to be actual answer objects.  $\square$

Consider the example shown in Fig. 1(a), where the green dotted circle denotes the search region, and the red solid circle denotes the ball region  $R_i = \{o_6, o_7, o_8\}$  with its center  $R_i.p = o_7$  and its radius  $R_i.r = d(o_7, o_6)$ . As  $d(q, R_i.p) < r - R_i.r$ ,  $R_i$  can be validated according to Lemma 3.6.

**LEMMA 3.7 (EXCLUSIVE VALIDATION).** Given a  $\rho$ -split function  $bps^\rho(c, o)$ , a query object  $q$ , and a search radius  $r$ , if  $bps^{\rho+r}(c, q) = 0$  (or 1), then the query result must be contained in  $R_0$  (or  $R_1$ ).

PROOF. If  $bps^{\rho+r}(c, q) = 0$ , then we can get that  $d(q, c) \leq d_{med} - \rho - r$ . For any object  $o$  outside  $R_0$  (i.e.,  $d(c, o) > d_{med} - \rho$ ),  $d(q, o) \geq d(o, c) - d(q, c) > d_{med} - \rho - d_{med} + \rho + r = r$ , and thus the query result must be contained in  $R_0$ ; If  $bps^{\rho+r}(c, q) = 1$ , then we can get that  $d(q, c) > d_{med} + \rho + r$ . For any object  $o$  outside  $R_1$  (i.e.,  $d(c, o) \leq d_{med} + \rho$ ),  $d(q, o) \geq d(q, c) - d(c, o) > d_{med} + \rho + r - d_{med} - \rho = r$ , and thus the query result must be contained in  $R_1$ . The proof completes.  $\square$

Consider the example shown in Fig. 1(c), and the search region is denoted as the green dotted circle. We can conclude that the search result must be contained in the hash partition region  $R_1$  due to  $bps^{\rho+r}(c, q) = 1$  according to Lemma 3.7. Hence, we only need verify the objects in  $R_1$ .

Table 3. Compact-partitioning based Metric Indexes

Partitioning Technique	Index	Storage	Scalability
Generalized hyperplane partitioning	GHT, GNAT	Main-memory	Static
	EGNAT	External-memory	Dynamic
	$k$ NNG	Main-memory	Dynamic
	M-Index	External-memory	Dynamic
Ball partitioning	M-tree and PM-tree	External-memory	Dynamic
	LC, DLC, HC	External-memory	Dynamic
Hash partitioning	D-index	External-memory	Dynamic
	MB <sup>+</sup> -tree	External-memory	Dynamic
Hybrid partitioning	BST, MBST, VT, BU-tree	Main-memory	Static
	SAT	Main-memory	Static
	HRG	Main-memory	Dynamic
	DSAT, DSACLT	External-memory	Dynamic
	TLAESA	Main-memory	Static

#### 4 Detailed Category of Metric Indexes

As stated in Section 2.3, metric indexes can be classified into two main categories, compact-partitioning based methods and pivot-based methods. The hybrid methods combines the two categories, which belong to both compact-partitioning based methods and pivot-based methods.

##### 4.1 Compact-Partitioning based Metric Indexes

Compact partitioning methods partition the space as compact as possible and try to prune unqualified partitions during search. They can be divided into four categories by the partitioning technique used, namely, *generalized hyperplane partitioning based indexes*, *ball partitioning based indexes*, *hash partitioning based indexes*, and *hybrid partitioning based indexes* as listed in Table 3.

Indexes in the first category uses the generalized partitioning technique defined in Definition 3.2 to partition the dataset. GHT is a binary tree constructed by using the generalized partitioning, which can be extended to the  $m$ -ary tree GNAT and the dynamic tree EGNAT.  $k$ NNG uses a graph structure to maintain the relationship between each object and its  $k$  nearest neighbors. M-index also uses the generalized hyperplane partitioning to build the index.

Indexes in the second category uses the ball partitioning technique defined in Definition 3.1 to partition the dataset. M-tree and its variants are external dynamic trees built using ball partitioning technique. Different from M-tree that use a tree structure, LC and DLC use a list structure to organize the ball regions. In addition, LC can be extended to a tree structure HC.

Indexes in the third category utilizes the hash partitioning technique defined in Definition 3.3 to divide the dataset. D-index uses the  $\rho$ -split function to recursively divide the dataset. MB<sup>+</sup>-tree uses the hash partitioning or the relaxed generalized partitioning to obtain the compact partitions and generate keys, which are then indexed by B<sup>+</sup>-tree.

Indexes in the fourth category combines the ball partitioning and hyperplane partitioning techniques. In particular, they use the hyperplane partitioning to divide the dataset, but use ball partitioning technique to represent each partition. BST and its variants (i.e., MBST, VT, BU-tree) use the combined partitioning technique to construct the binary tree. SAT follows the delaunay graph structure, which can be extended to dynamic versions (i.e., HRG, DSAT and DSACLT). TLAESA uses the combined partitioning technique to build the binary tree structure.

##### 4.2 Pivot-based Metric Indexes

Pivot-based methods store pre-computed distances from every object in the database to a set of pivots and then use those distances to prune objects during search. Pivot-based methods can

Table 4. Pivot-based Metric Indexes

Category	Index	Storage	Scalability
Pivot-based tables	AESA, ROAESA, iAESA	Main-memory	Dynamic
	LAESA	Main-memory	Dynamic
	EPT	Main-memory	Dynamic
	CPT	External-memory	Dynamic
Pivot-based trees	BKT	Main-memory	Dynamic
	FQT, FHQT, FQA	Main-memory	Dynamic
	TLAESA	Main-memory	Static
	GNAT	Main-memory	Static
	VPT, MVPT	Main-memory	Static
	DVPT	Main-memory	Dynamic
Pivot-based external indexes	PM-tree	External-memory	Dynamic
	EGNAT	External-memory	Dynamic
	D-index	External-memory	Dynamic
	Omni-family	External-memory	Dynamic
	M-index	External-memory	Dynamic
	SPB-tree	External-memory	Dynamic

be clustered into three categories, namely, *pivot-based tables*, *pivot-based trees*, and *pivot-based external indexes*, according to the structures they use for storing the pre-computed distances, as listed in Table 4.

Indexes in the first category utilize tables to store pre-computed distances. AESA and its variants ROAESA and iAESA use a table to preserve the distances from each object to other objects. To save main memory storage for the table, LAESA only keeps the distances from every object to selected pivots. EPT selects multiple sets of essential pivots covering the entire database, while CPT clusters the pre-computed distances to further improve query efficiency.

Indexes in the second category use tree structures to store pre-computed distances. BKT is designed for discrete distance functions. Different from BKT that uses different pivots at individual levels, FQT and its variants FHQT and FQA use the same pivot for all the nodes at the same tree level. GNAT is an  $m$ -way generalization of GHT, which utilizes the generalized hyperplane partition method to partition the dataset and also uses cut-regions defined by pivots to accelerate search. VPT is designed for continuous distance functions, as its dynamic version is VPT and its generalization to  $m$ -ary trees is called MVPT.

Indexes in the third category utilize an external index (e.g., the R-tree or the B<sup>+</sup>-tree) to store pre-computed distances. The Omni-family employs existing structures (e.g., the R-tree) to index pre-computed distances. The PM-tree stores cut-regions defined by pivots in each node of an M-tree to accelerate search. EGNAT is a dynamic version of GNAT that stores as a tree structure on the disk. The D-index combines the hash partitioning and the pivot mapping, where objects are stored as multi-level buckets on disk. The M-index uses the B<sup>+</sup>-tree to store pre-computed distances. The SPB-tree utilizes a space-filling curve to map pre-computed distances to integers, which are then indexed by the B<sup>+</sup>-tree.

According to Table 4, although many of the pivot-based methods are dynamic, all the indexes need to be re-built by re-computing all the stored distances when pivots are updated. However, the pivots do not need to be real objects in the dataset, and thus, the pivots are not necessary updated when we insert or delete data objects. Among all the metric indexes, only two of them (i.e., BKT and FQT) are designed for discrete distance functions, i.e., distance functions return finite values. However, they can be extended to support continuous distance functions.

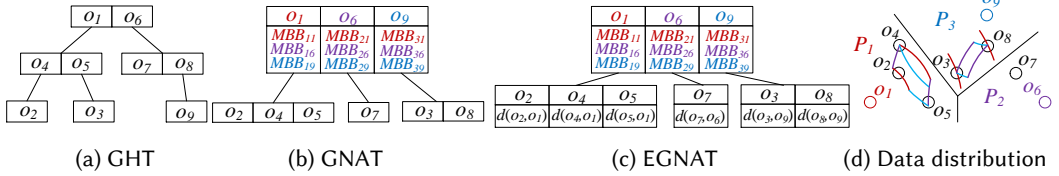


Fig. 3. Examples of GHT and its Variants

## 5 Metric Indexes for Exact Metric Similarity Search

In order to illustrate the detailed structures of all the metric indexes, we use the dataset shown in Fig. 1 as a running example to build different metric indexes.

### 5.1 GHT family

Generalized Hyperplane tree (GHT) is a binary tree built recursively by using generalized partitioning technique. An example of GHT is illustrated in Fig. 3(a). Each node contains two objects, where only leaf nodes can contain one object. Objects  $c_1$  and  $c_2$  in the node denote the centers of two subtrees. More specifically, if an object  $o$  is closer to  $c_1$ , then  $o$  is distributed to the subtree whose center is  $c_1$ , and vice versa.

GHT can be generalized to  $m$ -ary trees, yielding Generalized Near-Neighbor Access Tree (GNAT). An example of GNAT is depicted in Fig. 3(b). Each time,  $m$  centers  $c_i$  ( $1 \leq i \leq m$ ) are selected, and objects are distributed to the nearest center, resulting in  $m$  sub partitions/subtrees  $P_i$  ( $1 \leq i \leq m$ ), i.e., for any  $o \in P_i$  satisfying  $d(o, c_i) \leq d(o, c_j)$ . In addition, GNAT stores the minimum bounding box  $MBB_{ij} = [mindist(o, c_j), maxdist(o, c_j)]$  ( $o \in P_i$ ) of each partition  $P_i$  with respect to  $m$  centers  $c_j$ , which can help pruning during the search. The MBB information of GNAT is shown in Fig 3(d), where red circles denote the MBB information w.r.t. the center  $o_1$ , the purple circles denote the MBB information w.r.t. the center  $o_6$ , while the blue circle denotes the MBB information w.r.t. the center  $o_9$ . In this example, the second partition  $P_2$  only contains data  $o_7$ , and thus, the MBB information is omitted in the figure.

Evolutionary Geometric Near-neighbor Access Tree (EGNAT) is a dynamic version of GNAT, with an example shown in Fig. 3(c). It provides the insertion and deletion operations, as well as extends the main-memory index to the external index. In addition, to further improve the pruning ability, different GNAT, each entry in the leaf nodes of EGNAT stores additional distance from this entry to its parent entry (i.e., the center) of the corresponding leaf node.

**MRQ processing.** MRQ( $q, r$ ) processing using GHT is simple. We traverse the GHT in a depth-first manner. For each node, we use Lemma 3.3 (i.e., the double-pivot filtering) to filter unqualified nodes. If the node cannot be pruned, we compute the distance from the query object  $q$  and the center  $c$  of the node to determine whether the center  $c$  is the final result of MRQ( $q, r$ ). Specifically, if the unpruned node is a non-leaf node, we continue to visit its children; otherwise, we compute the distance between the query object and the non-center object in the leaf node, and determine whether the non-center object is the result of MRQ( $q, r$ ). For GNAT, due to additional minimum bounding box stored in each node, Lemma 3.1 can also be used for pruning when verifying each node. EGNAT stores the distances to its parent entry in leaf nodes, and thus, Lemma 3.2 is also used for pruning leaf entries.

**MkNNQ processing.** MkNNQ( $q, k$ ) processing based on GHT, GNAT, and EGNAT also follows the second approach introduced in Section 2.2. It initializes the search radius (the  $k$ -th nearest neighbor distance) to infinity, and the search radius is updated using candidate objects.

**Discussion.** The storage cost of GHT is  $O(ns)$  and its construction cost is  $\Omega(n \log_2 n)$ , while the storage cost of GNAT is  $O(ns + mn)$  and its construction cost is  $\Omega(mn \log_m n)$ , where  $n$  denotes the number of total objects,  $s$  denotes the size of an object, and  $m$  denotes the tree-arity. Here,  $O(mn)$

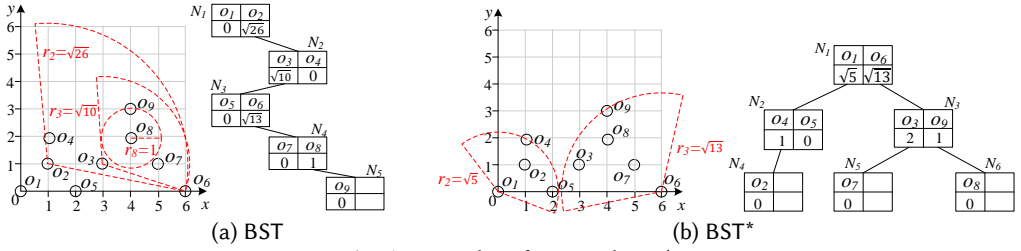


Fig. 4. Examples of BST and BST\*

is used to store the MBB information. Although EGNAT stores the distance between each leaf entry and its parent entry, its storage and construction cost complexity will not be affected. Note that, GHT, GNAT, and EGNAT are unbalanced trees, and thus, their worst construction cost is  $O(n^2)$ . In the best case, we assume that the tree structure is balanced, and thus, we can get an optimal construction cost  $\Omega(n \log_2 n)$  for GHT, and  $\Omega(mn \log mn)$  for GNAT and EGNAT.

## 5.2 BST family

BST is a binary tree that is similar to GHT. The only difference between GHT and BST is that, BST uses a ball (i.e., a center with a radius) to represent each partition/node, while GHT does not have the radius information in each node. BST is constructed by inserting the objects one by one. Fig. 4(a) gives an example of BST, where  $N_2$  is denoted using a ball whose center is  $o_2$  with the radius  $r_2$ . To improve the efficiency (i.e., to get a relatively balanced BST), BST can be built recursively in a top-down manner, called BST\*. In each node, we pick up two centers  $p_1$  and  $p_2$  for its sub nodes, and then distribute the left data in the node using the generalized hyperplane partitioning technique, i.e., distributing the data to the closer sub node. The partition starts from a root containing the whole dataset and stops when the node only two objects in a node. Fig. 4(b) gives an example of BST\*. In contrast, a variant BU-tree that builds the tree in a bottom-up manner instead of top-down manner. In BST, sub nodes could have larger radius than parent node. To avoid this, two variants MBST and VT are proposed, where VT is a 3-arity tree.

**MRQ processing.** MRQ( $q, r$ ) processing using BST is similar to GHT. The only difference is that BST uses Lemma 3.2 (i.e., the range-pivot filtering) instead of Lemma 3.3 to filter nodes.

**MkNNQ processing.** MkNNQ( $q, k$ ) processing based on BST follows the second strategy introduced in Section 2.2. It initializes the search radius (the  $k$ -th nearest neighbor distance) to infinity, and the search radius is updated using candidate objects.

**Discussion.** The storage cost of BST(\*) and MBST is  $O(ns)$  and the corresponding construction cost is  $\Omega(n \log_2 n)$ . As they are unbalanced trees, the balance depends on the chosen centers and data distribution. If we use well chosen centers, especially the two centers chosen for the root node, the BST and its variants will be balanced trees. Hence, the lower bound construction cost of BST(\*) and MBST is  $\Omega(n \log_2 n)$  if the tree structure is balanced. As VT tree is 3-arity tree, its construction cost is  $\Omega(n \log_3 n)$ . BU-Tree initializes each object as a node and each time it finds the two nodes with the minimum distance to merge, and thus, its construction cost is  $O(n^3)$ .

## 5.3 SAT family

Different from GNAT, Spatial Approximation Tree (SAT) selects the centers inspired by the Delaunay graph. An example of SAT is shown in Fig. 5(a). For each node  $c$ , SAT picks up a set of so-called nearest neighbors  $N(c)$  as the centers of its sub nodes. More specifically,  $N(c)$  does not denote the real nearest neighbors of  $c$ . In contrast,  $N(c)$  is defined as objects that are closer to  $c$  than other objects in  $N(c)$ , i.e.,  $o \in N(c)$  iff  $\forall u \in N(c) - \{o\}, d(o, p) < d(o, u)$ . In the sequel, same as GNAT, the generalized hyperplane partitioning is used, i.e., the objects are distributed to the closest corresponding subtree of  $o \in N(c)$ . Note that, the root node is randomly selected. Each node in SAT also uses the ball representation, i.e., a covering radius equaling to the maximum

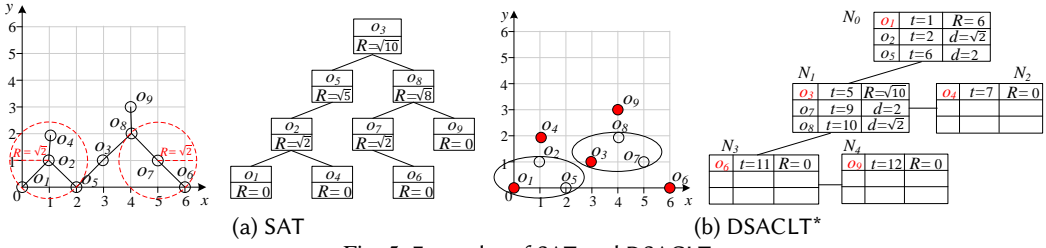


Fig. 5. Examples of SAT and DSACL T

distance between the node center and any object in the subtree is maintained with each node. To improve the efficiency of SAT, the fastest outlier data is selected as the root node instead of randomly choosing the root node in order to maximize the hyperplane separation [30]. In addition, when dividing the dataset in each iteration, all the data objects are sorting in ascending order of their distances to the parent entry. Another metric index termed  $k$  nearest-neighbor graph ( $k$ NNG) is similar to SAT. The only difference is that, SAT uses  $N(c)$  as sub nodes,  $k$ NNG uses real  $k$  nearest neighbors of  $c$  as its sub nodes.

Dynamic SAT (DSAT) extends SAT from a static in-memory index to a dynamic external index. For each node of DSAT, the number of sub nodes is limited to a given threshold MAXARY (i.e., the tree-arity). DSAT is built incrementally by inserting the object one by one, and each object is associated with a timestamp to indicate the insertion time. To insert a new object  $o$ , DSAT is traversed in a top-down manner to find the particular node  $c$  that  $o \in N(c)$ . As the number of sub nodes is limited to MAXARY, if the current number of sub nodes of  $o$  is smaller than MAXARY, then  $o$  is directly inserted as a sub node of  $c$ ; otherwise, it follows the generalized partitioning principle and is recursively inserted in the closet subtree of  $c$ . Note that, sub nodes are sorted in ascending order of insertion times.

To better clustering each page of DSAT, DSAT with clusters (DSACL T) is proposed, as depicted in Fig. 5(b). Each node of DSACL T is stored as a single page in the external memory. In addition, it finds and stores  $k$  nearest neighbors ( $k$ NNs) of the node center in each node. Note that, the distances from  $k$ NNs to the node center are also stored in each node. Two versions of DSACL T exist, including DSACL T<sup>+</sup> and DSACL T<sup>\*</sup>, where DSACL T<sup>+</sup> stores as a tree structure while DSACL T<sup>\*</sup> stores as a list. Similar as DSACL T, HRG finds and stores at most  $k$  NNs of the node center in each node. However, HRG is stored in main-memory, while DSACL T is stored on disk.

**MRQ processing using SAT.** MRQ( $q, r$ ) processing using SAT is similar to GHT. It traverses the SAT in a depth-first order. For each node, we first compute its distance the query object. If the distance is not larger than  $r$ , then we insert the node in the final result; Otherwise, Lemmas 3.2 and 3.3 are used to prune its sub nodes. Note that, instead of applying Lemma 3.3 only once for each sub node, all the sub nodes belonged to the same parent node and accessory nodes can be used for pruning. Let  $AN(o)$  be the accessory nodes of  $o$ . For each sub node  $o \in N(c)$ , if  $d(q, o) - d(q, u) > 2 \times r$  ( $u \in (N(c) - \{o\}) \cup AN(o)$ ), then the subtree of  $o$  can be pruned.

**MRQ processing using DSAT.** Different from MRQ( $q, r$ ) processing using SAT, DSAT cannot prune the whole subtree using Lemma 3.3. This is because, supposing that a node has two sub nodes  $c_i$  and  $c_j$  ( $j > i$ ), which means that  $c_i$  is inserted earlier than  $c_j$ , objects  $o$  inserted earlier before  $c_j$  in the subtree of  $c_i$  might belong to the subtree of  $c_j$ . Hence, we need to continue visiting older nodes even there exists a newer center satisfying the condition of Lemma 3.3.

**MRQ processing using DSACL T.** MRQ( $q, r$ ) processing using DSACL T is similar as that using DSAT. The only difference is that, for unpruned node, DSACL T determines whether the

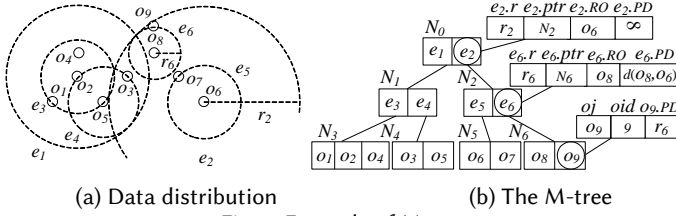


Fig. 6. Example of M-tree

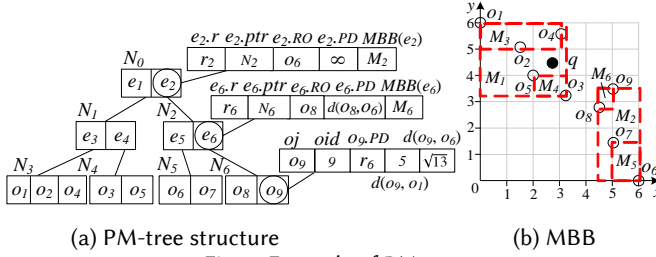


Fig. 7. Example of PM-tree

stored  $k$ NNs are in the final result by using Lemma 3.2. Note that, as discussed in Section 3.2, Lemma 3.2 can be extended to prune a single object with its pre-computed distance to the center.

**MkNNQ processing.** MkNNQ( $q, k$ ) processing using SAT also follows the second approach introduced in Section 2.2. The SAT is traversed in a best-first order, i.e., nodes are visited in ascending order of their minimum distances to the query object  $q$ . However, for DSAT and DSACLT, the nodes are visited in ascending order of insertion times, so that DSAT and DSACLT are traversed in depth-first order during MkNNQ( $q, k$ ) processing.

**Discussion.** The construction cost complexity of SAT, DSAT and DSACLT is  $O(n \log n / \log \log n)$ ,  $O(nm \log m)$ , and  $O(nm \log m^n / k)$  respectively, where  $m$  is maximum tree-arity and  $k$  denotes the number of nearest neighbors stored in each DSACLT nodes. The construction cost of HRG and  $k$ NNG is  $O(n^2)$ . The storage cost complexity of SAT,  $k$ NNG, DSAT, HRG, and DSACLT are the same  $O(ns)$ . Different from other indexes (e.g., GHT family) that only use sibling centers for pruning, SAT family can also use its ancestors for pruning, and thus, the pruning ability is stronger. Due to the dynamic insertions, the pruning ability of DSAT is weaker than SAT. For DSACLT, it stores more pre-computed distances in each node compared with SAT and DSAT, resulting in stronger pruning ability. However, the height of DSACLT is smaller than that of SAT and DSAT, resulting in weaker pruning ability. Hence, the whole pruning ability of DSACLT depends on the data distribution.

#### 5.4 M-tree family

M-tree is a dynamic tree. Fig. 6 shows an M-tree example. An intermediate (i.e., a non-leaf) entry  $e$  in a root node (e.g.,  $N_0$ ) or a non-leaf node (e.g.,  $N_1, N_2$ ) records the following. (i) A center  $e.RO$  that is a selected object in the subtree  $ST_e$  of  $e$ . (ii) A covering radius  $e.r$  that is the maximum distance between  $e.RO$  and the objects in  $ST_e$ . (iii) A parent distance  $e.PD$  that equals the distance from  $e$  to the center of its parent entry. Since a root entry  $e$  (e.g.,  $e_6$ ) has no parent entry,  $e.PD = \infty$ . (iv) An identifier  $e.ptr$  that points to the root node of  $ST_e$ . In contrast, a leaf entry (i.e., a data object)  $o$  in a leaf node (e.g.,  $N_3, N_4, N_5, N_6$ ) records the following. (i) An object  $o_j$  that stores the detailed information of  $o$ . (ii) An identifier  $oid$  that represents  $o$ 's identifier. (iii) A parent distance  $o.PD$  that equals the distance from  $o$  to the center of  $o$ 's parent entry.

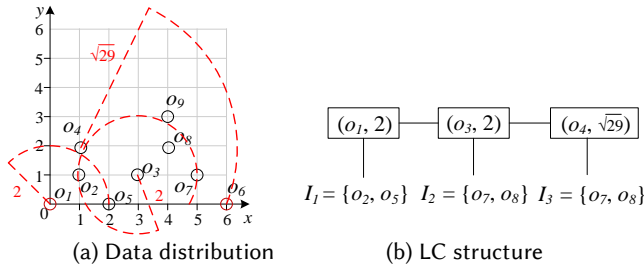


Fig. 8. Example of LC with fixed bucket size

Many variants of M-tree exist (as introduced in Section 2.3) that aim to improve its construction or query efficiency. Here, we only introduce a representative variant PM-tree below. The PM-tree combines the pivot mapping and the M-tree, where the M-tree is used to cluster the objects, and the pivot mapping is utilized to avoid unnecessary distance computations. Hence, different from the M-tree, each leaf entry of the PM-tree stores the mapped vector (i.e., the pre-computed distances to the pivots) with every object. In each intermediate entry, PM-tree stores the minimum bounding box (MBB) to contain all the mapped vectors in its child leaf entries. Fig. 7 illustrates an example of PM-tree.

**MRQ processing.** In order to answer  $\text{MRQ}(q, r)$  using M-tree, the entries are traversed in depth-first fashion. When an intermediate entry is accessed, we evaluate its qualifying child entries using Lemma 3.2; when a leaf entry is accessed, we insert the corresponding object into the result set if it is not discarded by Lemma 3.2.  $\text{MRQ}(q, r)$  using PM-tree is similar as that using M-tree, the only difference is that Lemma 3.1 can also be used for pruning entries due the pivot mapping technique.

**MkNNQ processing.**  $\text{MkNNQ}(q, k)$  using M-tree follows the second strategy discussed in Section 2.2. The entries are traversed in best-first manner, i.e., in ascending order of their minimum distances to the query object  $q$ , where Lemma 3.2 are employed to eliminate unqualified entries.  $\text{MkNNQ}(q, k)$  using PM-tree is similar to that using M-tree, and the only difference is that Lemma 3.1 can also be used for pruning entries.

**Discussion.** M-tree is a balanced tree, and thus, the construction cost of M-tree is  $O(nm \log_m n)$  with the storage cost  $O(ns + ns/m)$ . Note that, the tree-arity  $m$  of the M-tree depends on its disk page size to store each node. PM-tree stores additional pre-computed distances w.r.t. the pivots in the tree structure. Hence, the construction cost of PM-tree is  $O(n(m + l) \log_m n)$  and its storage cost is  $O(n(s + l) + n(s + l)/m + ls)$ , where  $l$  denotes the number of pivots, and it takes  $O(ls)$  to store the pivots. The PM-tree costs are relatively high compared with those of M-tree. The M-tree and its variants (e.g., PM-tree) store the data objects in its entries instead of in a separate file, and thus, the page/node size varies for different types of data. In particular, for complex objects (e.g., the 282 dimensional vectors used in our experiments), the M-tree family need a large page size.

## 5.5 LC family

List of Clusters (LC) is a list of clusters, where each cluster is represented by a center and a radius. In addition, each cluster has a corresponding bucket, which contains objects whose distances to the center are not larger than the radius. LC has two versions, i.e., fixed radius and fixed size. Fixed radius means that the cluster radius is fixed, while fixed size denotes that the number of objects in each bucket is fixed. Fig. 8 illustrates the example of LC with fixed size. Two variants Dynamic LC (DLC) and Hierarchy of Clusters (HC) are proposed, where DLC is a dynamic version of LC and HC is a tree structure to store the list of clusters.

**MRQ processing.**  $\text{MRQ}(q, r)$  using LC, DLC and HC is simple. It visits the list of clusters in sequel or visits the tree in depth-first order. If a cluster cannot be pruned by Lemma 3.2, then we

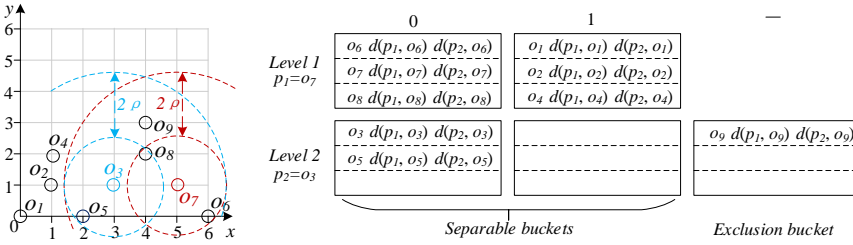


Fig. 9. Example of D-index

verify objects in the corresponding bucket. If the search region is contained in the ball cluster, the search can stop and the results can be returned, i.e., the clusters do not need to be visited.

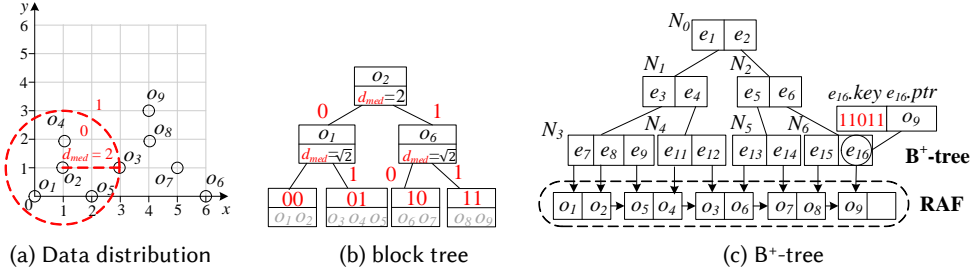
**MkNNQ processing.** MkNNQ( $q, k$ ) using LC, DLC and HC adopts the second strategy in Section 2.2, where Lemma 3.2 is used for pruning.

**Discussion.** The construction cost of LC and DLC is  $O(n^2/m)$ , where  $m$  denotes the number of objects contained in each bucket. Objects are easier to insert the first several clusters. The construction cost of LC is very high, however, it can achieve high query efficiency due to the compact clusters. HC is built recursively in binary way to reduce the construction cost of LC, and thus, its construction cost is  $O(n \log_2^n/m)$ . The storage size of LC, DLC and HC is  $O(ns)$ .

## 5.6 D-index family

D-index combines the hash partitioning method (i.e., excluded middle partitioning) and the pivot mapping technique. The basic idea of the D-Index is to create a multilevel structure that uses several  $\rho$ -split functions defined in Definition 3.3, one for each level, to create buckets for storing objects. On the first level, we use a  $\rho$ -split function for separating objects of the whole data set. For any other level, objects mapped to the exclusion bucket of the previous level are the candidates in separable buckets of this level. For example, in Fig. 9, objects in exclusion bucket ‘-’ (i.e.,  $o_3, o_5, o_9$ ) at level 1 are candidates to be divided in level 2. Finally, the exclusion bucket of the last level forms the exclusion bucket of the whole D-index. Here, the  $\rho$ -split functions of individual levels use the same  $\rho$ . Fig. 9 gives an example of D-index, where a  $\rho$ -split function based on  $o_7$  is used at level 1, and a  $\rho$ -split function based on  $o_3$  is used at level 2.

MB<sup>+</sup>-tree recursively divides the dataset into two sub-sets by using either hash partitioning technique or generalized hyperplane partitioning. Fig. 10 gives an example of MB<sup>+</sup>-tree using hash partitioning, where  $\rho$  is set to 0 when constructing MB<sup>+</sup>-tree. MB<sup>+</sup>-tree includes two parts, i.e., the block tree and the B<sup>+</sup>-tree. The block tree stores the partition information, where each internal node records the partition center  $c$  and the medium distance  $d_{med}$  used for a  $\rho$ -split function. Since  $\rho$  is set to 0 for MB<sup>+</sup>-tree, only two buckets (i.e., bucket 0 and bucket 1) are got after hashing. For example, in Fig. 10, according to the red circle centered at  $o_2$  with  $d_{med} = 2$ , the whole dataset are divided into two sub sets  $\{o_1, o_2, o_3, o_4, o_5\}$  and  $\{o_6, o_7, o_8, o_9\}$ . The leaf node of the block tree denotes a partition and is associated with a partition key. For each object  $o$ , MB<sup>+</sup>-tree generates a key that includes the partition key  $pk$  and the distance key  $dk$ . The partition key can be easily derived using the path from the partition node to the root, where the left sub-tree can be denoted as ‘0’, where the right sub-tree is denoted as ‘1’, as shown in Fig. 10(b). The distance key  $dk$  is a bit string to denote  $\lfloor (2^{nk} - 1)(R + d(o, c))/2R \rfloor$  based on the distance  $d(o, c)$  between the object  $o$  and its block center  $c$ , where  $R$  denotes the maximum distance and  $nk$  is the number of bits to represent the maximum distance. As shown Fig. 10(c), assuming that the maximum distance  $R$  is 6,  $nk$  equals to 3 in order to represent the whole distance range. Then, the key of object  $o_9$  is ‘11011’, where ‘11’ is the partition key and ‘011’ is the distance key. Here, ‘011’ = 5 is used to denote the lower bound distance  $\lfloor (2^3-1)(8+d(o_9, o_6))/16 \rfloor$ . Finally, all the keys are indexed by B<sup>+</sup>-tree, and objects are stored in a separated random access file RAF.

Fig. 10. Example of MB<sup>+</sup>-tree by using hash partitioning

**MRQ processing using D-index.** The D-index is visited in a top-down manner. For each level, we use Lemma 3.4 to prune the unqualified buckets and search the result in the unpruned buckets. In addition, if Lemma 3.7 satisfies, then we can directly search the final result in the corresponding bucket and terminate the search. Note that, during searching the result in each bucket, Lemma 3.1 is used for pruning to improve the efficiency.

**MRQ processing using MB<sup>+</sup>-tree.** MRQ( $q, r$ ) using MB<sup>+</sup>-tree visits the block tree in depth-first order, where Lemma 3.7 is used to find sub-trees that needs to be visited. When a leaf node of the block tree reaches whose center is  $c$ , it computes the distance key range for query object  $q$  (i.e., the minimum distance key  $\lfloor (2^{nk} - 1)(d(q, c) + R - r)/2R \rfloor$  and the maximum distance key  $\lfloor (2^{nk} - 1)(d(q, c) + R + r)/2R \rfloor$ ). Then it finds in B<sup>+</sup>-tree all the candidates belonged to this leaf node and fall in this distance key range, and then determines whether each candidate is the final result.

**MkNNQ processing using D-index.** MkNNQ( $q, k$ ) using D-index is complex. We can adopt the second solution discussed in Section 2.2. However, instead of setting the search radius to infinity initially, we first set the search radius to  $\rho$ , and then search the  $k$  NNs. If the upper bound distance between current  $k$  NNs and the query object is larger than  $\rho$  (i.e., the initial search radius  $\rho$  is underestimated), we need to search the D-index again to refine the result.

**MkNNQ processing using MB<sup>+</sup>-tree.** MkNNQ( $q, k$ ) using MB<sup>+</sup>-tree adopts the third strategy in Section 2.2. It first finds  $k$  candidate NNs according to the keys, i.e., finding  $k$  candidates with their keys nearest to the query object's key, and then calculates the current  $k$ -th NN distance  $ND_k$  using the  $k$  candidates. After that, MkNNQ( $q, k$ ) is transformed to a metric range search MRQ( $q, ND_k$ ) to find the final result.

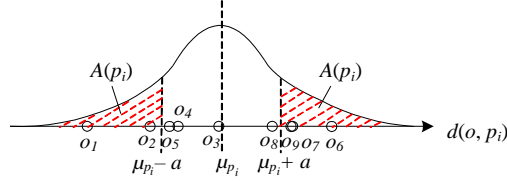
**Discussion.** The construction cost of D-index is  $O(nl)$ , as it depends on the number of pivots (i.e., the number of hash functions) used. The storage cost of D-index is  $O(ns + nl + ls)$ , where  $O(ns)$  is the cost to store the dataset,  $O(nl)$  is cost to store the pre-computed distances w.r.t. the pivots, and  $O(ls)$  is the cost to store the pivots used for pivot mapping and hash partitioning. The construction cost of MB<sup>+</sup>-tree is  $O(n \log_2^n/m + nm \log_m n)$ , where it takes  $O(n \log_2^n/m)$  to build the block tree and  $O(nm \log_m n)$  to build the B<sup>+</sup>-tree, where  $m$  denotes the number of entries for both block tree leaf node and B<sup>+</sup>-tree node. The storage cost of MB<sup>+</sup>-tree is  $O((n+n/m)(s + \log_2^n/m + \log_2 n_d))$ , where  $n_d$  denotes the maximum distance value of  $d$ . This is because, the length of partition key is  $O(\log_2^n/m)$  while the length of distance key is  $O(\log_2 n_d)$ . It takes  $O((n+n/m)(\log_2^n/m + \log_2 n_d))$  to store B<sup>+</sup>-tree,  $O(ns)$  to store RAF, and  $O((s + \log_2^n/m)n/m)$  to store the block tree.

## 5.7 AESA family

AESA uses a table to store the distances from every object to other objects. If  $n$  is the cardinality of a dataset, then the storage cost of AESA is  $O(n^2)$ , which is high for large datasets. As an example, if  $n = 100,000$ , the storage cost is 80G. That renders AESA a theoretical metric index. To further improve the query efficiency, two variants ROAESA and iAESA are proposed, where the pre-computed distances are sorted and visited in a particular order. To reduce the storage cost of

object	$d(o_i, o_1)$	$d(o_i, o_6)$
$o_1$	0	6
$o_2$	$\sqrt{2}$	$\sqrt{26}$
$o_3$	$\sqrt{10}$	$\sqrt{10}$
$o_4$	$\sqrt{5}$	$\sqrt{29}$
$o_5$	2	4
$o_6$	6	0
$o_7$	$\sqrt{26}$	$\sqrt{2}$
$o_8$	$2\sqrt{5}$	$2\sqrt{2}$
$o_9$	5	$\sqrt{13}$

Fig. 11. Example of LAESA

Fig. 12. Illustration of  $A(p_i)$ 

object	$(p_1, d(o_i, p_1))$	$(p_2, d(o_i, p_2))$
$o_1$	$(o_1, 0)$	$(o_9, 5)$
$o_2$	$(o_1, \sqrt{2})$	$(o_4, 1)$
$o_3$	$(o_1, \sqrt{10})$	$(o_9, \sqrt{5})$
$o_4$	$(o_6, \sqrt{29})$	$(o_4, 0)$
$o_5$	$(o_1, 2)$	$(o_9, \sqrt{13})$
$o_6$	$(o_6, 0)$	$(o_4, \sqrt{29})$
$o_7$	$(o_6, \sqrt{2})$	$(o_4, \sqrt{17})$
$o_8$	$(o_1, 2\sqrt{5})$	$(o_9, 1)$
$o_9$	$(o_1, 5)$	$(o_9, 0)$

Fig. 13. Example of EPT

AESA, Linear AESA (LAESA) is proposed. LAESA only stores the distances from each object to the pivots in a pivot set  $P$ . Fig. 11 shows an example of LAESA when using the pivot set  $P = \{o_1, o_6\}$ . In addition, the objects in LAESA can be organized in a binary tree TLAESA instead of a table.

**MRQ processing.** MRQ( $q, r$ ) processing using LAESA is simple. We compute the distances  $d(q, p_i)$  between the query object  $q$  and the pivots  $p_i (\in P)$  and then verify the objects in the dataset  $O$  one by one. For every object  $o$  in  $O$ , if it cannot be pruned by Lemma 3.1, we compute  $d(q, o)$  and insert  $o$  into the result set if  $d(q, o) \leq r$ .

**MkNNQ processing.** MkNNQ( $q, k$ ) processing based on LAESA follows the second strategy introduced in Section 2.2. It initializes the search radius to infinity, and computes the distances from the query object  $q$  to the pivots in  $P$ . Subsequently, objects in the dataset  $O$  are verified one by one. For each object  $o$ , if it cannot be pruned by Lemma 3.1, we compute  $d(q, o)$  and update the search radius using the current  $k^{\text{th}}$  nearest neighbor distance.

**Discussion.** The construction cost of AESA and ROAESA is  $O(n^2)$ , while the construction cost of iAESA is  $O(n^2 \log_2 n)$  to sort the pre-computed distances. The storage cost of AESA, ROAESA and iAESA is  $O(ns + n^2)$ , as they take  $O(ns)$  to store the data and  $O(n^2)$  to store the pre-computed distances. To reduce the cost of AESA, the construction cost of LAESA is  $O(nl)$  and its storage cost is  $O(ns + nl + ls)$ , as LAESA takes  $O(ns)$  to store the data,  $O(nl)$  to store the pre-computed distances, and  $O(ls)$  to store pivots. As TLAESA is a tree structure, the construction cost of TLAESA is  $O(n \log_2 n + nl)$ , but its storage cost is same as LAESA. For similarity search processing, although LAESA utilizes Lemma 3.1 to avoid certain unnecessary distance computations, it still needs to scan the full table to find the result set, which incurs additional scanning cost.

## 5.8 EPT

Unlike LAESA that utilizes the same pivots for each object, Extreme Pivot Table (EPT) selects different pivots for different objects in order to achieve better search performance.

EP consist of a set of pivot groups. Each group  $G$  contains  $g$  pivots  $p_i (1 \leq i \leq g)$ , according to which the whole dataset  $O$  is partitioned into  $g$  parts  $A(p_i)$ , such that  $A(p_i) \cap A(p_j) = \emptyset (i \neq j)$  and

**Algorithm 1** Pivot Selecting Algorithm (PSA)

---

**Input:** a set  $O$  of objects, the number  $l$  of pivots for each object  
**Output:** EPT\*  
1: obtain a sample set  $S$  from  $O$   
2:  $CP = \text{HF}(O, cp\_scale)$  // get a candidate pivot set  $CP$  ( $|CP| = cp\_scale$ )  
3: **for** each object  $o$  in  $O$  **do**  
4:    $P = \emptyset$   
5:   **while**  $|P| < l$  **do**  
6:     select a different  $p_i$  from  $CP$  to maximize  $\sum_{o' \in S} D(o', o)/d(o', o)$   
7:      $P = P \cup \{p_i\}$   
8:   update EPT\* with  $\langle (p_1, d(o, p_1)), (p_2, d(o, p_2)), \dots, (p_l, d(o, p_l)) \rangle$   
9: **return** EPT\*

---

$\cup_{p_i \in G} A(p_i) = O$ . An object  $o$  belongs to  $A(p_i)$  iff  $|d(o, p_i) - \mu_{p_i}| \geq \alpha$ , where  $\mu_{p_i}$  is the expected value of  $d(o, p_i)$ . For example, in Fig. 12,  $A(p_i) = \{o_1, o_2, o_7, o_9, o_6\}$ .

However, it is hard to obtain  $\alpha$ , and hence, EPT tries to maximize  $\alpha$ . In other words, EPT randomly selects  $g$  pivots as a pivot group  $G_j$ , and sets the pivot  $p_i$  in  $G_j$  to an object  $o$  having  $\max\{d(o, p_i) - \mu_{p_i} \mid p_i \in G_j\}$ . The processing is repeated  $l$  times, i.e.,  $l$  groups  $G_j$  ( $1 \leq j \leq l$ ) are selected. Thus, each object has corresponding  $l$  pivots. Fig. 13 depicts an example of EPT. Let  $g = 2$  and  $l = 2$ , two pivot groups are selected at random, i.e.,  $G_1 = \{o_1, o_6\}$  and  $G_2 = \{o_4, o_9\}$ . The structure of EPT is similar to that of LAESA. However, since each object in EPT may have different pivots, EPT stores the corresponding pivot (i.e., the *id* of the pivot) with the pre-computed distances.

Let  $X = d(p_i, o)$  and  $Y = d(p_i, q)$ , then the query cost in terms of the number of distance computations can be estimated as:

$$\begin{aligned} cost &= g \times l + |O| \times (1 - \Pr(|X - Y| > r))^l \\ &\geq g \times l + |O| \times \left(1 - \frac{\sigma_x^2 + \sigma_y^2}{r^2}\right)^l \end{aligned} \quad (2)$$

Using Equation 2, we can approximate the optimal  $g$  by fixing  $l$  (to control the main-memory storage size), where  $\sigma_x^2$ ,  $\sigma_y^2$ , and  $r$  can be estimated. Nevertheless, EPT utilizes  $Z = d(o, q)$  to estimate  $Y = d(p_i, q)$ , which is inaccurate. In addition, it is difficult to estimate  $r$  that is specified by the user.

We therefore proceed to introduce a new pivot selection algorithm (PSA) to improve the efficiency of EPT. Let  $D(q, o) = \max\{|d(q, p_i) - d(o, p_i)| \mid p_i \in P\}$ , which is a lower bound of  $d(q, o)$  according to the triangle inequality. Hence, the query cost can be estimated as:

$$cost = g \times l + |O| \times \Pr(D(q, u) > r) \quad (3)$$

To achieve the optimal query cost defined in Equation 3,  $D(q, u)$  should approach  $d(q, o)$  as much as possible in order to avoid unnecessary distance computations of  $d(q, o)$ . Thus, PSA tries to select a pivot set that maximizes the random variable  $D(q, o)/d(q, o)$ .

Algorithm 1 presents the pseudo-code of PSA. First, it samples the object set  $O$  as set  $S$ , and invokes HF algorithm [66] to obtain outliers as candidate pivots  $CP$  (lines 1-2). Here,  $cp\_scale$  is set to 40 because this value yields enough outliers in our experiments. Then, for each object  $o$  in  $O$ , the algorithm incrementally selects effective pivots from  $CP$  that maximize  $D(q, o)/d(q, o)$  (lines 4-7), and updates EPT\* (line 8). Finally, EPT\* is returned (line 9).

**MRQ and M $k$ NNQ processing.** Like LAESA, EPT and EPT\* use tables to store pre-computed distances. The only difference is that EPT and EPT\* utilize different pivots for different objects, while LAESA uses the same pivots for every object. Hence, MRQ and M $k$ NNQ processing on EPT or EPT\* are the same as those on LAESA.

**Discussion.** The construction cost of EPT is  $O(nlg)$ , while the storage cost of EPT is  $O(nl + ns + lgs)$ , as EPT takes  $O(ns)$  to store the real data,  $O(nl)$  to store the pre-computed distances, and

pointer	$d(o_i, o_1)$	$d(o_i, o_6)$
$o_1$	0	6
$o_2$	$\sqrt{2}$	$\sqrt{26}$
$o_3$	$\sqrt{10}$	$\sqrt{10}$
$o_4$	$\sqrt{5}$	$\sqrt{29}$
$o_5$	2	4
$o_6$	6	0
$o_7$	$\sqrt{26}$	$\sqrt{2}$
$o_8$	$2\sqrt{5}$	$2\sqrt{2}$
$o_9$	5	$\sqrt{13}$

Fig. 14. Example of CPT

$O(lgs)$  to store the pivots. EPT has  $l$  groups while each group contain  $g$  pivots, and thus, it takes  $O(lgs)$  to store all the pivots. For each object, we will select a best pivot among each pivot group, and thus, it takes  $O(nl)$  to store the pre-computed distances between objects and best pivots. To get higher quality pivots for each object, the construction cost of EPT\* is  $O(nll_cn_s)$ , where  $l_c$  denote the number of candidate pivots and  $n_s$  denotes the cardinality of the sample set. The storage cost of EPT\* is  $O(ns + nl + l_cs)$ , as EPT\* takes  $O(ns)$  to store the real data,  $O(nl)$  to store the pre-computed distances, and  $O(l_cs)$  to store all the pivots. EPT\* achieves a better similarity search performance than EPT contributed by the higher quality pivots selected by PSA. Nonetheless, it is costly to maximize  $\sum_{o' \in S} D(o', o)/d(o', o)$ , and thus, the construction cost of EPT\* is very high.

### 5.8 CPT

LAESA and EPT store the distance table and the data file in main memory, and similarity query processing needs to scan the whole table. However, when the size of the dataset exceeds the capacity of the main memory, it is necessary to store the dataset on disk, and it becomes attractive to cluster the data to improve I/O efficiency.

The CPT uses an M-tree to cluster and store the objects on disk. The CPT consists of two parts, i.e., the distance table (depicted in Fig. 14) and the M-tree (depicted in Fig. 6). The distance table stores the pre-computed distances between objects and the selected pivots in main memory. The M-tree includes the objects stored on disk (i.e., each M-tree leaf entry contains one object). Note that, the distance table includes the pointers to the leaf entries in the M-tree, in order to enable loading of the corresponding objects for verification.

**MRQ and M $k$ NNQ processing.** MRQ and M $k$ NNQ processing using CPT are similar to the processing using LAESA. The only difference is that, when an object cannot be pruned using Lemma 3.1, the object must be read from disk.

**Discussion.** The construction cost of CPT is  $O(mn \log_m n + nl)$ , as it takes  $O(mn \log_m n)$  to build the M-tree and  $O(nl)$  to construct the table. The storage cost of CPT is  $O(ns + ns/m + nl + ls)$ , as it takes  $O(ns + ns/m)$  to store the M-tree,  $O(nl)$  to store the pre-computed distances, and  $O(ls)$  to store the pivots. Using CPT, we can avoid loading the whole dataset into main memory to perform query processing. However, CPT incurs the I/O cost to load objects from disk. In addition, the distance table is stored in main memory, meaning that the applicability of CPT is still limited to datasets for which the distance table fits in main memory.

### 5.9 BKT

BKT is a tree structure designed for discrete distance functions. It chooses a pivot as the root, and maintains the objects having the distance  $i$  to the pivot in its  $i^{\text{th}}$  sub-tree. If a sub-tree contains more than one objects, it selects a pivot at random and partitions the sub-tree recursively. Fig. 15

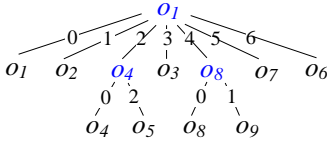


Fig. 15. Example of BKT

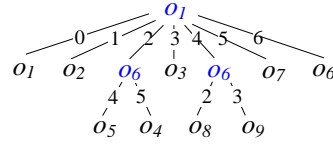


Fig. 16. Example of FQT

gives an example BKT, constructed based on the objects from Fig. 1 and the discrete distance function  $L_\infty$ -norm. However, for other metric index examples, Euclidean distance ( $L_2$ -norm) is used. The leaf nodes store the actual objects, while the non-leaf nodes store the corresponding pivots used to partition the sub-trees. Although BKT is designed for discrete distance function, the continuous distance range can be partitioned into discrete ranges used for indexing. For example, if the continuous distance function range is  $[0, 30]$ , we can divide it into three disjoint ranges  $[0, 10]$ ,  $[10, 20]$ ,  $[20, 30]$  in order to simulate the discrete distance function. Hence, BKT can be adapted to support both discrete and continuous distance functions.

**MRQ processing.** In order to answer  $\text{MRQ}(q, r)$ , the nodes in the BKT are traversed in depth-first fashion. When a non-leaf node is accessed, we identify its qualifying child entries using Lemma 3.1; when a leaf node is accessed, we insert the corresponding object into the result set if it is not pruned by Lemma 3.1.

**MkNNQ processing.** In order to answer  $\text{MkNNQ}(q, k)$ , the nodes in the BKT are traversed in best-first manner, i.e., in ascending order of their minimum distances to the query object  $q$ , where Lemma 3.1 is used to filter out unqualified nodes. Here, we first set the search radius to infinity and then update it using the visited objects, which follows the second strategy in Section 2.2.

**Discussion.** BKT is an unbalanced tree. The construction cost of BKT is  $O(nl)$ , where  $l$  denotes the height of BKT. To compare different pivot-based metric methods, we need to use same number of pivots, and thus, the height of BKT is set to  $l$  in this paper. However, we cannot use the same set of pivots for BKT as other pivot-based methods, BKT randomly selects the pivots for sub-trees. If BKT uses the same pivots as other pivot-based metric indexes, it produces FQT as discussed below. The storage cost of BKT is  $O(ns + ln_d)$ , where  $n_d$  denotes the number of discrete values in the domain of distance function  $d()$ . To avoid empty sub-trees for large distance domains, each sub-tree covers a range of distance values, which are stored together.

### 5.10 FQ family

Unlike BKT, FQT utilizes the same pivot at the same level. Fig. 16 shows an example of FQT, where  $o_1$  is used for the first level, and  $o_6$  is used for the second level. FQT is also an unbalanced tree. Hence, FHQT is proposed, where objects are stored in the leaves and all the leaves are at the same level. In addition, FHQT can be also stored as FQA using an array/table structure. Note that, FQA and LAESA are the same. Although FQT is designed for discrete distance function, it can also be extended to support continuous distance function similar as BKT.

**MRQ and MkNNQ processing.** MRQ and MkNNQ processing using FQT are the same as for BKT.

**Discussion.** The construction cost of FQT is  $O(nl)$ , and the storage cost of FQT is  $O(ns + nl)$ , where  $l$  denotes the height of FQT. This is because, in order to utilize the same set  $P$  of pivots as other pivot-based metric indexes, the height of FQT is set to the number of pivots, and  $p_i \in P$  is set as the pivot for the  $i^{\text{th}}$  level. With well-chosen pivots, the performance of FQT is expected to be better than that of BKT.



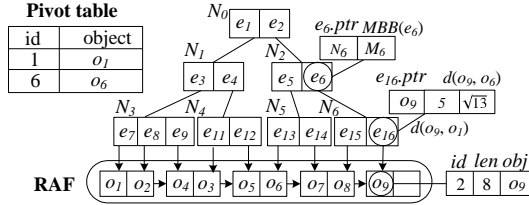


Fig. 18. Example of OmniR-tree

3.1; when a leaf entry is accessed, we compute the actual distance and insert the corresponding object into the result set if the distance is no larger than  $r$ .

**MkNNQ processing.** To answer  $MkNNQ(q, k)$ , the entries in the R-tree are traversed in best-first manner, i.e., in ascending order of their minimum distances to the query object  $q$ , where Lemma 3.1 is used to prune unqualified entries. By following the second strategy discussed in Section 2.2, we set the search radius to infinity and then update it using the visited objects.

**Discussion.** The Omni-family includes the Omni-sequential-file, the OmniB<sup>+</sup>-tree, and the OmniR-tree. Omni-sequential-file can be regarded as LAESA stored on disk, which incurs substantial I/O during search as the data is not clustered. The OmniB<sup>+</sup>-tree needs one B<sup>+</sup>-tree for each pivot, resulting in redundant storage and I/O during search. The OmniR-tree utilizes MBBs to cluster the data, and uses the pivot filtering to achieve high query efficiency. The construction cost of OmniR-tree is  $O(nl + nm \log_m n)$ , as it takes  $O(nl)$  to do the pivot mapping and takes  $O(nm \log_m n)$  to build the R-tree. The storage cost of OmniR-tree is  $O(ns + nl + nl/m + ls)$ , where it takes  $O(ns)$  to store the real data in RAF,  $O(nl + nl/m)$  to store the pre-computed distances in R-tree, and  $O(ls)$  to store the pivots in pivot table.

### 5.13 M-Index

The M-index combines the generalized hyperplane partitioning and the pivot mapping. Given a set  $P$  of pivots, each object  $o$  is assigned to the partition of its nearest pivot  $p_i$  ( $i \in P$ ), and is mapped to the real number  $key(o) = d(p_i, o) + (i - 1) \times n_d$ , where  $n_d$  is the maximum distance in a certain metric space. Considering the example in Fig. 19(a), if  $P = \{o_1, o_6\}$ , we obtain two clusters  $C_1$  and  $C_2$ . After the partitioning, a cluster tree (as depicted in Fig. 19(b)) is used to maintain the information of the clusters (i.e., the minimum and maximum mapped numbers  $minkey$  and  $maxkey$ , the minimum bounding box MBB), a B<sup>+</sup>-tree is used to index the mapped real numbers, and an RAF is used to store the objects with pre-computed distances to all the pivots. If more pivots are used, the cluster-tree can be extended to a dynamic tree, as shown in Fig. 19(d). Specifically, if the number of the objects in a certain cluster exceeds a threshold  $maximum$  (set to 1,600 in this paper), the cluster can be further partitioned using the left pivots.

**MRQ processing using M-index.** To answer  $MRQ(q, r)$ , the entries in the cluster tree are traversed in depth-first fashion. When an intermediate entry is visited, we evaluate its qualifying child entries using Lemma 3.3; when a leaf entry is accessed, we obtain the objects that belong to this cluster from B<sup>+</sup>-tree, and filter out the unqualified objects according to Lemma 3.1.

**MkNNQ processing using M-index.** To answer  $MkNNQ(q, k)$ , by taking the first strategy discussed in Section 2.2, a range query with a small search radius is performed first, and then, the search radius is increased gradually until  $k$  closest objects are found.

**MRQ and MkNNQ processing using M-index\*.** M-index\* adds the MBB information for each cluster in the M-index. Based on the MBBs, the pivot filtering technique Lemma 3.1 can be applied when traversing the cluster-tree in order to filter unqualified clusters in advance. In addition, the data validation technique Lemma 3.5 can also be integrated to avoid unnecessary

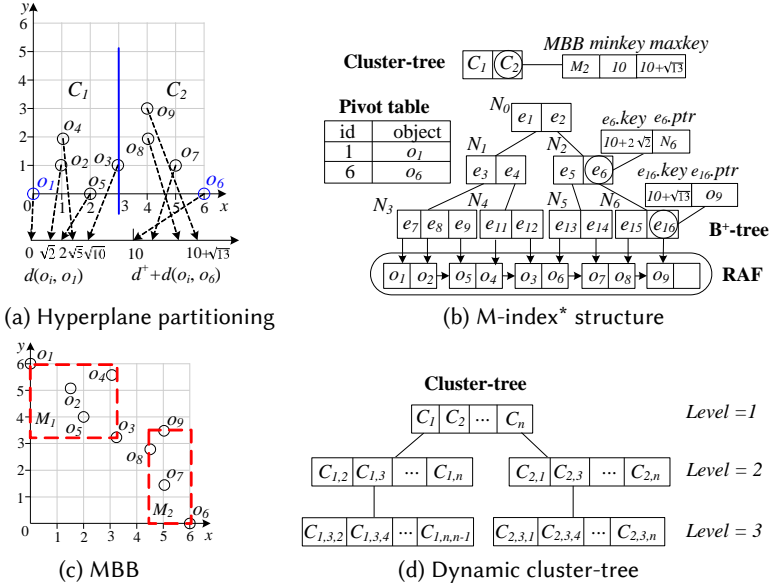


Fig. 19. Example of M-index\*

verifications. To answer  $MkNNQ(q, k)$ , M-index\* can use the second strategy instead of the first strategy based on the MBBs. More specifically, it traverses the cluster-tree in best-first manner, i.e., clusters are visited in ascending order of their distances to the query object  $q$ .

**Discussion.** The construction cost of M-index is  $\Omega(nl \log_i n/m + mn \log_m n)$ . Here, we need an optimal  $\Omega(nl \log_i n/m)$  cost to construct the dynamic unbalanced cluster tree and  $O(mn \log_m n)$  to construct B<sup>+</sup>-tree, where  $m$  denotes the number of entries in each cluster or each B<sup>+</sup>-tree mpde. The storage cost of M-index is  $O(ns + nl + n + n/m + ls)$ , as it needs  $O(ns + nl)$  cost to store RAF,  $O(n + n/m)$  cost to store B<sup>+</sup>-tree,  $O(n/m)$  cost to store cluster tree, and  $O(ls)$  cost to store the pivot table. By integrating the MBB information in the cluster tree, the storage of M-index\* is increased to  $O(ns + nl + n + n/m + nl/m + ls)$ . However, the efficiency of MRQ and  $MkNNQ$  performed on M-Index\* is improved. Since the M-index\* can use both Lemma 3.1 and Lemma 3.3 for pruning, it can achieve high performance in terms of distance computations. However, it needs to visit B<sup>+</sup>-tree multiple times for all unpruned clusters, and thus, the I/O performance is relatively high.

#### 5.14 SPB-Tree

The SPB-tree utilizes the two-stage mapping, i.e., the pivot mapping and the space-filling curve (SFC) mapping, to map objects into SFC values (i.e., integers) while (to some extent) maintaining spatial proximity. Then, a B<sup>+</sup>-tree is used to store the SFC values. Fig. 20 depicts an example of SPB-tree, where Fig. 20(b) illustrates the Hilbert mapping after the pivot mapping. In addition, each non-leaf entry  $e$  in B<sup>+</sup>-tree stores the SFC values  $min$  and  $max$  for  $\langle a_1, a_2, \dots, a_n \rangle$  and  $\langle b_1, b_2, \dots, b_n \rangle$  to represent the minimum bounding box information  $e.MBB = \{[a_i, b_i] \mid 1 \leq i \leq n\}$ .

**MRQ processing.** To answer  $MRQ(q, r)$ , the entries in the B<sup>+</sup>-tree are traversed in depth-first fashion. When an intermediate entry is visited, we identify its qualifying child entries using Lemma 3.1; when a leaf entry is accessed, we utilize Lemma 3.5 or compute the actual distance to validate the object.

**MkNNQ processing.** To answer  $MkNNQ(q, k)$ , the entries in the B<sup>+</sup>-tree are traversed in best-first manner, i.e., in ascending order of their minimum distances to the query object  $q$ , where

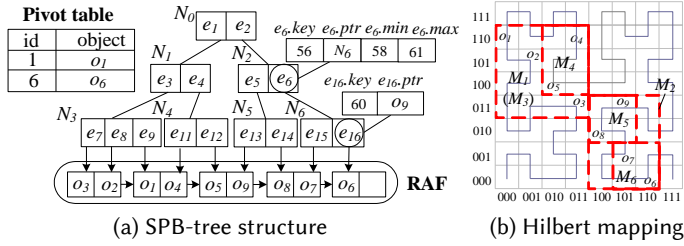


Fig. 20. Example of SPB-tree

Lemma 3.1 is used to filter unqualified entries. Following the second strategy discussed in Section 2.2, we set the search radius to infinity and then update it using the visited objects.

**Discussion.** The construction cost of SPB-tree is  $O(nlx + nm\log mn)$ , where  $x$  denotes the space filling curve transformation cost for each object. In particular, SPB-tree takes  $O(nlx)$  to do the pivot mapping and the space filling curve mapping, and takes  $O(nm\log mn)$  to build the  $B^+$ -tree. The storage cost of SPB-tree is  $O(ns + n + n/m + ls)$ , as it takes  $O(ns)$  to store the real data in RAF,  $O(n + n/m)$  to store the mapped values in  $B^+$ -tree, and  $O(ls)$  to store the pivot table. We employ the SFC mapping to reduce the storage cost and maintain spatial proximity at the same time, resulting in improved I/O and index storage costs. However, for continuous distance functions, the continuous distances are approximated as the discrete ones to perform the SFC mapping, which decreases the pruning power. In addition, during the similarity search, we need to do the Hilbert transformation to get the pre-computed distances, and thus, additional CPU cost is needed.

## 6 Experimental Comparison among Metric Indexes

As discussed in Section 2.2, it is hard to analyze the search performance based on the metric indexes, and thus, we experimentally compare 19 representative metric indexes, including BST (belonged to BST family), GNAT and EGNAT (belonged to GHT family), SAT and DSACLT (belonged to SAT family), M-tree and PM-tree (belonged to M-tree family), LC (belonged to LC family),  $MB^+$ -tree and D-index (belonged to D-index family), LAESA (belonged to AESA family), EPT\*, CPT, BKT, FQT (belonged to FQ family), MVPT (belonged to VPT family), OmniR-tree (belonged to Omni-family), SPB-tree and M-index\*. We implemented all the indexes and associated similarity search algorithms in C++. All experiments were conducted on an Intel Core i7-7700 3.6GHz PC with 16GB memory.

We employ three real datasets, namely *LA*, *Words*, and *Color*. *LA*<sup>1</sup> consists of geographical locations in Los Angeles, and the  $L_2$ -norm is utilized to measure similarity. *Words*<sup>2</sup> contains proper nouns, acronyms, and compound words taken from the Moby project, and the edit distance is used to compute the distances between words. *Color*<sup>3</sup> consists of standard MPEG-7 image features extracted from Flickr, and the similarity between two features is measured by the  $L_T$ -norm. A synthetic dataset is also created, where five dimension values are generated randomly, and the remaining dimension values are linear combinations of the previous ones. In order to study the performance of BKT and FQT that are designed for discrete distance functions, the values in the Synthetic dataset are generated as integers. Without loss of generality, the  $L_\infty$ -norm is employed for the Synthetic dataset. Table 5 summarizes the statistics of the datasets.

We investigate the similarity query performance of the indexes when varying the parameters listed in Table 6. The value of the radius  $r$  denotes the percentage of objects in the dataset that are

<sup>1</sup> *LA* is available at <http://www.dbs.informatik.uni-muenchen.de/~seidl>.

<sup>2</sup> *Words* is available at <http://icon.shef.ac.uk/Moby/>.

<sup>3</sup> *Color* is available at <http://cophir.isti.cnr.it/>.

Table 5. Datasets used in the Experiments

Datasets	Cardinality	Dimensionality	Measurement
<i>LA</i>	1,073,727	2	$L_2$ -norm
<i>Words</i>	611,756	1~34	Edit distance
<i>Color</i>	1,000,000	282	$L_1$ -norm
<i>Synthetic</i>	1,000,000	20	$L_\infty$ -norm

Table 6. Parameter Setting

Parameter	Values	Default
<i>Number of pivots <math>l</math></i>	3, 5, 10, 15, 20	5
<i>Search radius <math>r</math> (% of the maximum distance)</i>	2%, 4%, 8%, 16%, 32%	8%
<i>Number of <math>k</math></i>	5, 10, 20, 50, 100	20

result objects of a metric range query. In each experiment, one parameter is varied, and the others are fixed at their default values. As discussed in Section 2.2, the main performance metrics include the number of page accesses (*PA*), the number of distance computations (*compdists*), and the running time. Each measurement we report is an average over 100 random queries.

In addition, when comparing the performance of different pivot-based methods, the use of different pivot selection strategies renders the comparison of pivot-based indexing techniques challenging. For example, the OmniR-tree [66] utilizes HF algorithm to select outliers as pivots, while the SPB-tree uses HFI algorithm to select pivots that maximize the similarity between the original metric space and the vector space achieved by using the pivots. Since the performance of similarity query processing depends highly on the pivots used [5, 24], we use the same pivot selection strategy for the pivot-based indexes. More specifically, all pivot-based metric indexes utilize the same set of pivots selected by HFI algorithm [33, 37]. This does, however, not apply to EPT\*, BKT and GNAT family. As discussed in Sections 5.1, 5.8, and 5.9, GNAT uses centers in the same level as pivots, EPT\* utilizes different pivots for different objects, while BKT needs to randomly select pivots in its sub-trees.

### 6.1 Comparison among main-memory based metric indexes

In this subsection, we compare the performance of all the main-memory based metric indexes using MRQ and M $k$ NN queries. It includes compact-partitioning based indexes (i.e., BST and SAT), pivot-based indexes (i.e., LAESA, EPT\*, BKT, FQT, and MVPT), and hybrid index GNAT. When comparing the pivot-based indexes and compact partitioning based indexes, the pruning ability of pivot-based indexes and compact-partitioning based methods depend on the number of pivots and the number of centers, respectively. Hence, in this set of experiments, we set the number of pivot-based indexes equaling to the height of compact-partitioning based methods. Then, the number of pivots equals to the number of centers used for pruning each object in either pivot-based methods or compact-partitioning methods. GNAT and MVPT are multi-arity trees. Here, we set arity to 5 by comparing among a set of values and choosing the best value.

Fig. 21 and Fig. 22 show the MRQ and M $k$ NN performance (i.e., *compdists* and the running time) on four datasets, respectively. Here,  $k$  is set to 20 for M $k$ NN query, while  $r$  is fixed to 8% for metric range query. The first observation is that, the query cost (including the number of distance computations and the running time) first drops and then keeps stable or increases when the number of pivots or the tree height increase. This is because, the more pivots/the higher of tree structure, the stronger pruning ability. In addition, the more pivots, the more additional CPU cost to filter the search space. Hence, the best number of pivots for each metric index depends on the distance distribution of dataset and the structure of metric index. Table 7 summarizes the performance metric (including *Compdists* and the running time) ranking of all main-memory based metric indexes on four datasets using MRQ and M $k$ NN queries.

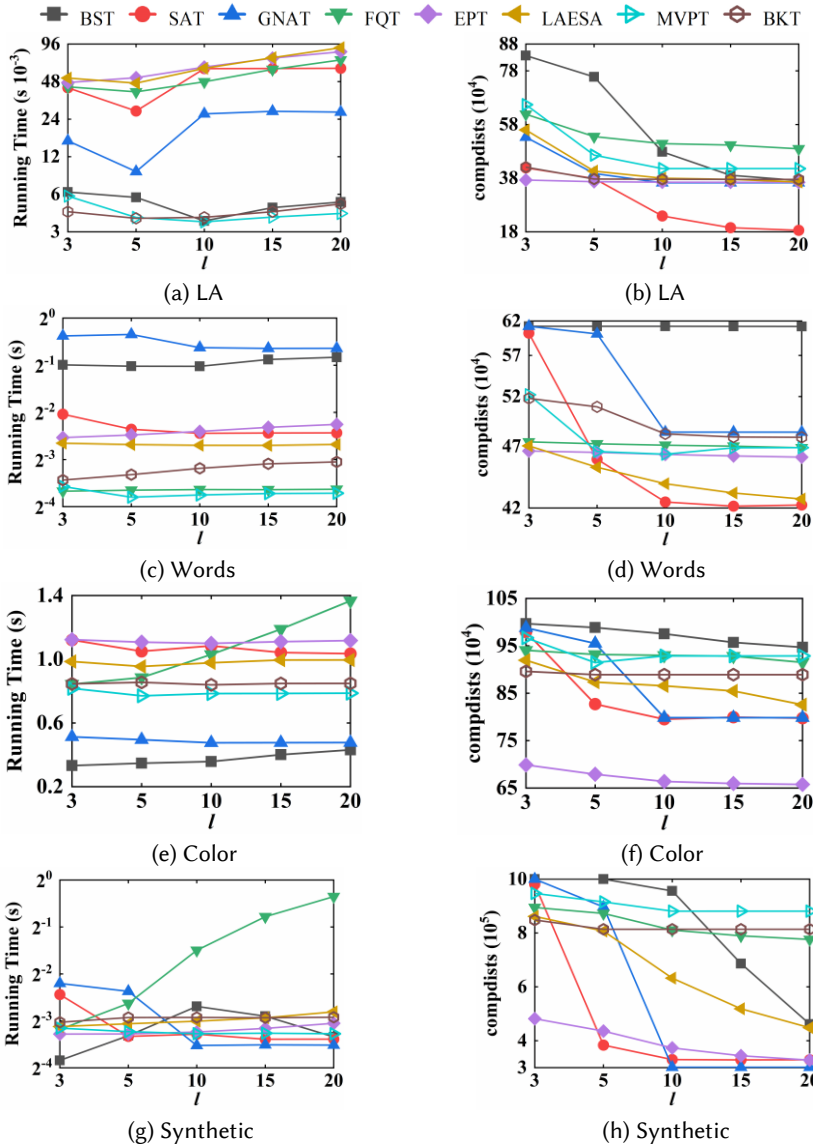


Fig. 21. Main-Memory based Metric Index Comparison Using MRQ queries

**Compdicts Performance Analysis.** As summarized in Table 7, SAT, EPT\* and GNAT achieve best performance in terms of distance computations, while BST and FQT perform worst. The number of distance computations depends on the selected pivots and the pivot based filtering and validation techniques associated with the metric structure. However, for fair comparison among index structures, we use the same set pivots for all the metric indexes except EPT\* and BST as stated in the settings. Hence, the reasons behind the distance computation performance observation are: 1) EPT\* selects different pivots for each object in order to get higher pruning ability, while other indexes take the same set of pivots for all objects in the dataset; 2) GNAT is a hybrid metric index that use two different pivot-based filtering techniques, and thus, can achieve better pruning ability; 3) SAT utilizes its ancestors for pruning while the others only use the centers at the same level for pruning, and thus, having higher pivot-based pruning ability; 4) BST

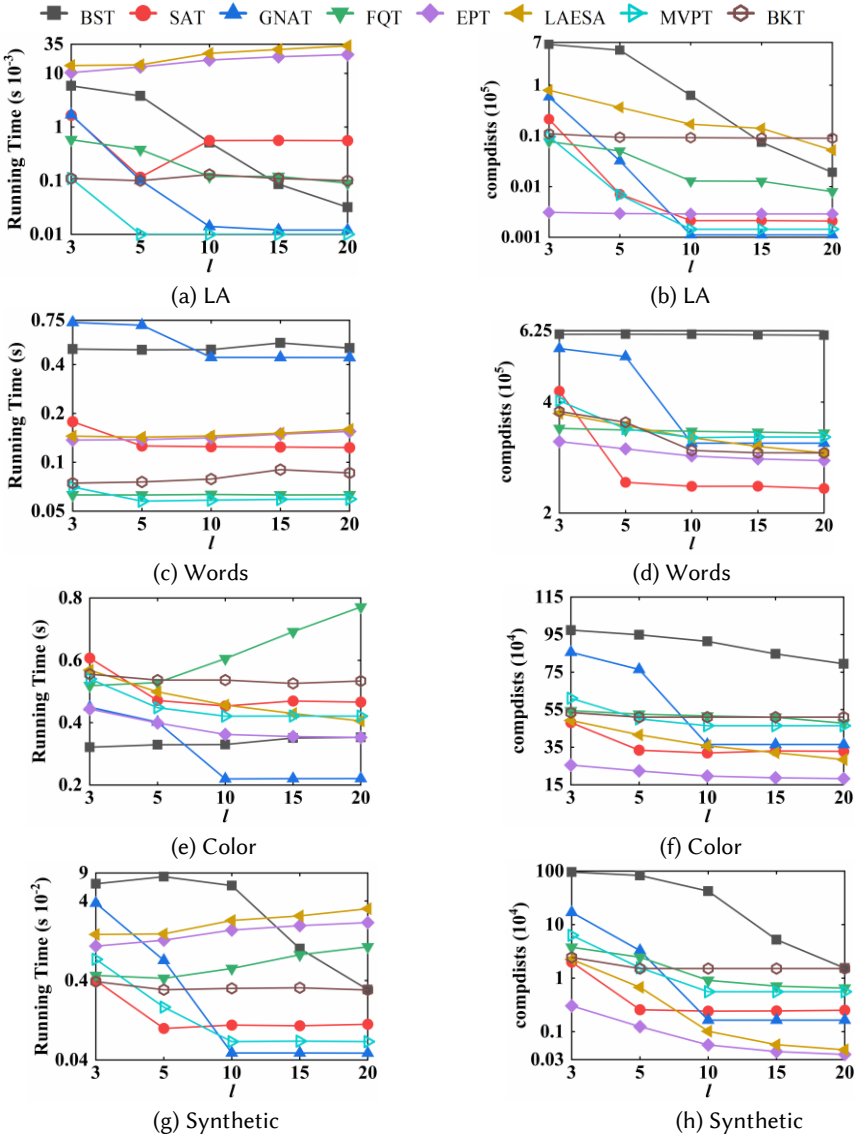


Fig. 22. Main-Memory based Metric Index Comparison Using MkNN queries

uses random pivots, and thus, its pivot filtering ability is weak; and 5) FQT is a unbalanced tree, and thus, less pivots are used for pruning. As stated in previous work, the pivot-based metric indexes can achieve better performance in terms of distance computations compared with compact partitioning based methods. However, if we use the same set of pivots and the same pruning and validation techniques, the number of distance computations between these two categories will be the similar. The reason why the distance computation performance of pivot-based metric indexes better is that they (e.g., LAESA, EPT\*) can support unlimited number of pivots, while the pivot number for compact partitioning methods is limited by the size of dataset (i.e., if few data is left, no further partition/no additional center is needed to build the index).

**CPU Performance Analysis.** As summarized in Table 7, MVPT and GNAT achieve best performance in terms of running time, while LAESA and EPT\* perform worst. Although LAESA and EPT\* achieve good performance in terms of distance computations, their CPU performance

Table 7. Main-memory-based Metric Indexes Ranking

Main-memory based Metric Index	<i>Compdists</i> ranking		Running time ranking	
	MRQ	MkNN	MRQ	MkNN
BST	8	8	3	7
SAT	1	2	5	4
LAESA	4	3	7	8
EPT*	2	1	7	6
BKT	5	6	4	3
FQT	7	7	6	5
MVPT	6	5	1	1
GNAT	3	3	2	2

Table 8. Disk-based metric Indexes Ranking

Disk-based Metric Index	PA ranking		<i>Compdists</i> ranking		Running time ranking	
	MRQ	MkNN	MRQ	MkNN	MRQ	MkNN
LC	1	1	1	5	1	1
DSACLT	3	3	5	7	2	4
M-tree	9	7	9	9	4	5
MB <sup>+</sup> -tree	5	8	10	11	9	11
OmniR-tree	6	5	8	2	7	2
SPB-tree	2	2	5	3	6	5
D-index	4	4	10	10	3	7
EGNAT	11	8	2	7	10	10
PM-tree	10	6	2	3	5	3
CPT	8	10	7	6	10	8
M-index	7	11	4	1	8	9

is bad. This is because, they are tables and the queries need to scan the whole table to find the final result without any bulk pruning. For the tree structure, MVPT and GNAT achieve better CPU performance as they are balanced trees while the others (SAT, BKT and FQT) are unbalanced. For BST, although it is balanced tree, the corresponding CPU cost is high because it is a binary tree and its pruning ability is weak. Hence, the CPU performance not only depends on the number of distance computations needed during the search, but also relies on the index structure.

## 6.2 Comparison among disk-based metric indexes

In this subsection, we compare the performance of all disk-based metric indexes using MRQ and MkNN queries. It includes compact-partitioning based methods (i.e., DSACLT, LC, MB<sup>+</sup>-tree and M-tree), pivot-based methods (i.e., OmniR-tree and SPB-tree), and hybrid methods (i.e., D-index, EGNAT, PM-tree, CPT, and M-index). For disk-based indexes (including B<sup>+</sup>-tree, R-tree and M-tree, etc.), the height of tree depends on the page/node size. Here, we fix the page size to 4KB, and the height of disk-based indexes can be calculated based on its structure and according to the data distribution. However, CPT, M-tree, PM-tree, LC and EGNAT store the real objects directly in the index structures. Thus, they need a large page size for high-dimensional data, and they are configured to use a fixed disk page size of 40KB on the Color and Synthetic datasets as default, while the others are configured to use a fixed disk page size of 4KB. However, a 40KB page size can also be regarded 10 4KB pages for one tree node or cluster. In addition, the number of pivots is fixed to 5, and all the pivot-based methods and hybrid methods (except EGNAT) use the same set of pivots for fair comparisons. This is because, EGNAT uses the centers as the level as the pivots due to its design.

Fig. 23 and Fig. 24 show the performance of disk-based metric indexes over four datasets using MRQ and MkNN queries, respectively. As expected, the query cost (including PA, *compdists*, and

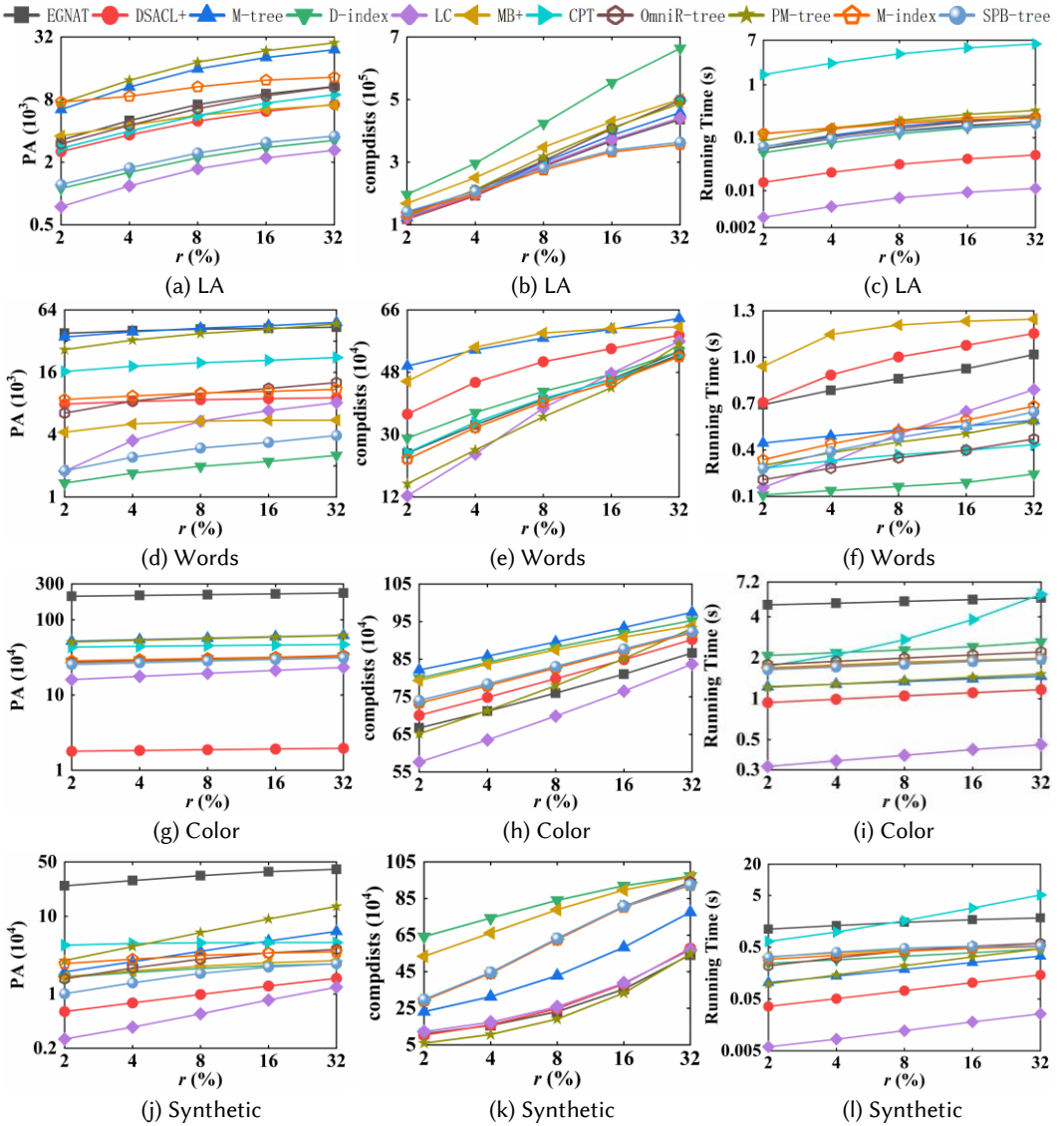


Fig. 23. Disk-based Metric Index Comparison Using MRQ queries

running time) increases with the growth of  $k$  and  $r$  value due to the larger search space. Table 7 gives the performance metric (including PA, *Compdist*s, and running time) ranking of all disk-based metric indexes over four datasets using MRQ and M $k$ NN queries. In the following, we give the ranking analysis of three different performance metrics, respectively.

**I/O performance analysis.** As summarized in Table 8, LC, SPB-tree and DSACL+ achieve best performance in terms of PA, followed by D-index, OmniR-tree, MB $^+$ -tree, and PM-tree, while EGNAT, CPT, and M-index perform worst. The I/O cost depends on two factors, including whether the data is well clustered and *compidists* needed during the search. Compact-partitioning based methods can achieve better I/O performance compared with pivot-based methods and hybrid methods, because compact-partitioning methods can well cluster the data and the pivot-based methods and hybrid ones need to store additional large number of pre-computed distances.

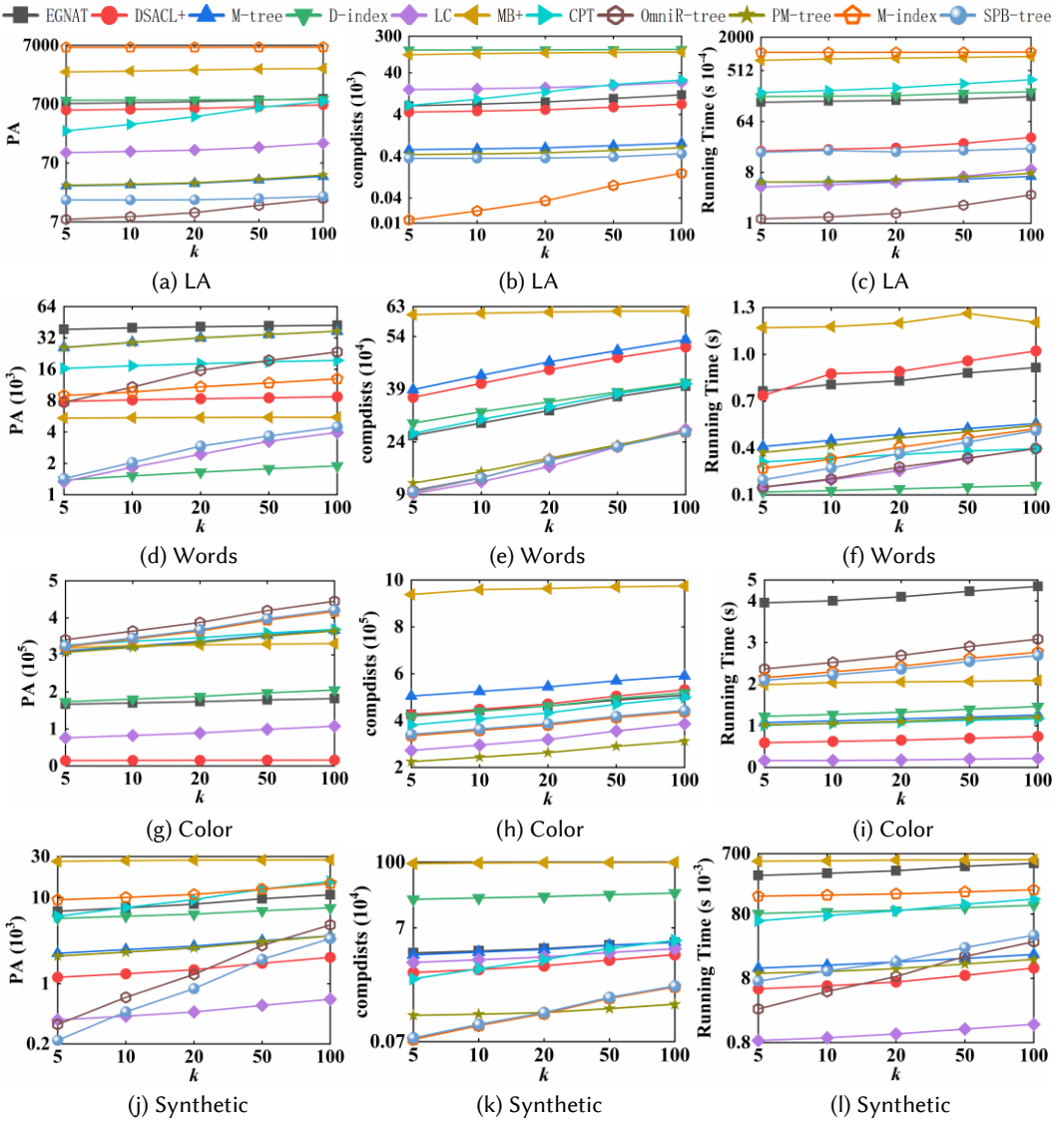


Fig. 24. Disk-based Metric Index Comparison Using MkNN queries

As LC and DSACL are partitioning-based methods that can well cluster the data, they can achieve good I/O performance. However, for M-tree and MB<sup>+</sup>-tree, although they cluster data in compact partitions, the *compdists* is high during the search (i.e., the pruning ability is weak). For SPB-tree, it is a pivot-based method, however it uses space-filling curve to cluster the data and highly reduce the storage of pre-computes. Thus, SPB-tree can archive good I/O performance.

**Compdists performance analysis.** As summarized in Table 8, M-index, OmniR-tree, SPB-tree and PM-tree achieve best performance in terms of *compdists* by considering MkNN queries, while LC, EGNAT and PM-tree perform best by considering MRQ queries. The disk-based metric index performance is slightly different using two different types of queries, because the search radius for MkNN queries is very small, while the search radius of MRQ is large in our experiments. More specifically, LC is constructed and searched in order of data occurrences, while others can search

in best-first order to find  $k$  NNs as soon as possible to shrink the search better. Hence, LC is better for MRQ with large search radius compared with  $Mk$ NN queries with small search radius. Overall, the pivot-based methods and hybrid ones can achieve better *compdists* performance compared with compact-partitioning methods. This is because we choose high quality pivots for pivot-based and hybrid methods, while the pruning ability of centers in compact-partitioning methods is weak. Note that, the construction cost of LC (one of compact-partitioning methods) is  $O(n^2)$ , which can well cluster the data to trade construction cost for query performance. However, the construction cost of LC is too high especially the cardinality of dataset  $n$  is very large, and thus, it is not a good choice. For D-index, although it is a hybrid method and uses pre-computed distances to prune the search space, the hashing partitioning is hard to control the quality of clusters, which depends on the split parameter  $\rho$  and the search radius.

**Overall performance analysis.** The running time of a query is used to evaluate the overall performance, which includes the CPU cost and I/O cost. The CPU cost includes two parts, i.e., the distance computation cost (*compdists*) and the filtering cost during search. Hence, the overall performance (i.e., the running time) depends on three factors, including PA, *compdists* and the additional CPU cost for pruning. As summarized in Table 8, LC, DSACLT and PM-tree achieve best performance in terms of running time, followed by M-tree, OmniR-tree, SPB-tree, and D-index, while MB<sup>+</sup>-tree, EGNAT, CPT and M-index perform worst. Here, LC, DSACLT and PM-tree have good overall performance, because they perform well on both PA and *compdists*. For M-index and EGNAT, although they have good *compdists* performance, their overall performance is not good due to high I/O cost during search. Although SPB-tree shows good performance on both PA and *compdists*, it needs additional CPU cost (i.e., space filling curve transformation) during the search, resulting in relatively high CPU cost compared to LC and DSACLT and PM-tree.

## 7 CONCLUSIONS

In this survey, we have introduced all the metric indexes that aim to accelerate exact similarity search, which can be classified into three categories, i.e., pivot-based methods, compact-partitioning based methods, and hybrid methods. Pivot-based methods store the pre-computed distances between well selected pivots and data objects, where three data structures (including table, tree, and external index) can be used. Thus, pivot-based indexes can be further divided into three types according to the data structure used to store pre-computed distances. Compact-partitioning based methods use four partitioning techniques (including ball partitioning, hyperplane partitioning, hash partitioning, and hybrid partitioning) to cluster the data, and thus, compact-partitioning based methods can be further divided into four types according to the partitioning technique used to cluster the data.

We have summarized all the punning and validation techniques based on pivots or centers to accelerate the similarity search using metric indexes. In addition, we have analyzed time and space complexity for metric index construction, and have conducted experimental analysis to evaluate metric index performance by using similarity search. The resulting findings and insights, summarized below, enable users to select the indexes that best support the intended uses:

- 1) For small datasets without considering the scalability, the main-memory based metric indexes can be chosen.
  - a. For complex distance computation functions (i.e., distance computation cost is the dominate CPU cost), EPT\*, SAT and GNAT are best choices, where SAT has the least construction cost, followed by GNAT, and EPT\* has the highest construction cost.
  - b. For simple distance computation function, MVPT and GNAT are best choices, where the construction of MVPT is more efficient compared with GNAT.
- 2) For large datasets considering the scalability, the disk-based metric indexes can be chosen.
  - a. For complex distance computation functions, SPB-tree, OmniR-tree and PM-tree are best choices. Because they can achieve good performance in terms of *compdists* and

have relatively good I/O performance. Note that, LC is not recommended here due to its huge construction cost for large datasets.

- b. For simple distance computation functions, DSCALT, D-index and PM-tree are best choices. Because they can achieve good performance in terms of PA, have relatively good *compdists* performance and need little additional CPU cost for pruning.

Although we have many metric indexes proposed to deal with the variety of big data, a number of open issues require further attention. Some possible future directions of metric indexes are summarized below:

- 1) The search space pruning is based on pivots for pivot-based metrics, while it is based on centers for compact-partitioning based metrics. To improve the search space pruning ability, it is of interest to study how to select high quality pivots or centers, especially for compact-partitioning based methods.
- 2) To further improve the performance of metric indexes, intelligent metric indexing can be considered by integrating the machine learning techniques. In addition, the distributed platform and the approximation optimizations can also be used.
- 3) As metric spaces only utilize the common triangle inequality to accelerate the search, possible directions of further work are how to improve the search efficiency by integrating specific characteristic of metric data and how to achieve high search efficiency if the triangle inequality is not satisfied for some distance functions.
- 4) With the demanding on public expectation of privacy increases, privacy concerns exist wherever personally identifiable information or other sensitive information is collected, stored, used, and finally destroyed or deleted. Hence, the last but not the least direction of future work is to protect the data privacy in metric indexes.

## 8 ACKNOWLEDGMENTS

This work was supported in part by the National Key Research and Development Program of China under Grant No. 2018YFB1004003, the NSFC under Grants No. 61972338, 61902343, and 61522208, the NSFC-Zhejiang Joint Fund under Grant No. U1609217, and the DiCyPS project. Yunjun Gao is the corresponding author of the work.

## REFERENCES

- [1] J. Almeida, R. D. S. Torres, and N. J. Leite. 2010. BP-tree: An efficient index for similarity search in high-dimensional metric space. In *CIKM*, 1365–1368.
- [2] J. Almeida, E. Valle, R. D. S. Torres, and N. J. Leite. 2010. DAHC-tree: An effective index for approximate search in high-dimensional metric spaces. *Journal of Information and Data Management* 1, 3 (2010), 375.
- [3] G. Amato, C. Gennaro, P. Savino. 2014. MI-file: Using inverted files for scalable approximate similarity search. *Multimedia Tools and Applications* 71, 3 (2014), 1333–1362.
- [4] F. Angiulli, and F. Fabio. Indexing uncertain data in general metric spaces. 2012. *IEEE Transactions on Knowledge and Data Engineering* 24, 9 (2012): 1640–1657.
- [5] L. G. Ares, N. R. Brisaboa, M. F. Esteller, O. Pedreira, and A. S. Places. 2009. Optimal pivots to minimize the index size for metric access methods. In *SISAP*, 74–80.
- [6] L. G. Ares, N. R. Brisaboa, A. O. Pereira, and O. Pedreira. 2012. Efficient similarity search in metric spaces with cluster reduction. In *SISAP*, 70–84.
- [7] L. Aronovich and I. Spiegler. 2007. CM-tree: A dynamic clustered index for similarity search in metric databases. *Data & Knowledge Engineering*, 63, 3 (2007), 919–946.
- [8] V. Athitsos, J. Alon, S. Sclaroff, and G. Kollios. 2007. Boostmap: An embedding method for efficient nearest neighbor retrieval. *IEEE Transactions on Pattern Analysis and Machine Intelligence*, 30, 1 (2007), 89–104.
- [9] V. Athitsos, M. Potamias, P. Papapetrou, and Kollios, G. 2008. Nearest neighbor retrieval using distance-based hashing. In *ICDE*, 327–336.
- [10] R. A. Baeza-Yates, W. Cunto, U. Manber, and S. Wu. 1994. Proximity matching using fixed-queries trees. In *CPM*, 198–212.
- [11] R. A. Baeza-Yates. 1997. Searching: An algorithmic tour. *Encyclopedia of Computer Science and Technology* 37 (1997), 331–359.

- [12] M. Barroso, N. Reyes, and R. Paredes. 2010. Enlarging nodes to improve dynamic spatial approximation trees. In *SISAP*, 41–48.
- [13] N. Beckmann, H. P. Kriegel, R. Schneider, and B. Seeger. 1990. The R\*-tree: An efficient and robust access method for points and rectangles. In *HPCS*, 322–331.
- [14] J. L. Bentley. 1975. Multidimensional binary search trees used for associative searching. *Communications of the ACM*, 18, 9 (1975), 509–517.
- [15] K. Beyer, J. Goldstein, R. Ramakrishnan, and U. Shaft. 1999. When is “nearest neighbor” meaningful? In *ICDT*, 217–235.
- [16] A. Beygelzimer, S. Kakade, and J. Langford. 2006. Cover trees for nearest neighbor. In *ICML*, 97–104.
- [17] C. M. Bishop. 2006. *Pattern Recognition and Machine Learning*. Springer-Verlag.
- [18] T. Bozkaya and M. Ozsoyoglu. 1997. Distance-based indexing for high-dimensional metric spaces. In *SIGMOD*, 357–368.
- [19] T. Bozkaya and M. Ozsoyoglu. 1999. Indexing large metric spaces for similarity search queries. *ACM Transactions on Database Systems* 24, 3 (1999), 361–404.
- [20] S. E. Bratsberg and M. L. Hetland. 2012. Dynamic optimization of queries in pivot-based indexing. *Multimedia Tools and Applications* 60, 2 (2012), 261–275.
- [21] S. Brin. 1995. Near neighbor search in large metric spaces. In *VLDB*, 574–584.
- [22] L. Britos, A. M. Printista, and N. Reye. 2012. DSACL+-tree: A dynamic data structure for similarity search in secondary memory. In *SISAP*, 116–131.
- [23] W. Burkhard and R. Keller. Some approaches to best-match file searching. *Communications of the ACM* 16, 4 (1973), 230–236.
- [24] B. Bustos, G. Navarro, and E. Chavez. 2003. Pivot selection techniques for proximity searching in metric spaces. *Pattern Recognition Letters* 24, 14 (2003), 2357–2366.
- [25] B. Bustos and T. Skopal. 2006. Dynamic similarity search in multi-metric spaces. In *Proceedings of the 8th ACM SIGMM International Workshop on Multimedia Information Retrieval*, 137–146.
- [26] D. Cantone, A. Ferro, A. Pulvirenti, D. R. Recupero, and D. Shasha. 2005. Antipole tree indexing to support range search and  $k$ -nearest neighbor search in metric spaces. *IEEE Transactions on Knowledge and Data Engineering* 17, 4 (2005), 535–550.
- [27] C. C. M. Carélo, I. R. V. Pola, R. R. Ciferri, A. J. M. Traina, C. T. Jr., and C. D. A. Ciferri. 2011. Slicing the metric space to provide quick indexing of complex data in the main memory. *Information Systems* 36, 1 (2011), 79–98.
- [28] E. Chávez and G. Navarro. 2000. An effective clustering algorithm to index high dimensional metric spaces. In *Proceedings of the 6th International Symposium on String Processing and Information Retrieval*, 75–86.
- [29] E. Chávez, K. Figueroa, and G. Navarro. 2008. Effective proximity retrieval by ordering permutations. *IEEE Transactions on Pattern Analysis and Machine Intelligence* 30, 9 (2008), 1647–1658.
- [30] E. Chávez, V. Ludueña, N. Reyes, and P. Roggero. 2016. Faster proximity searching with the distal SAT. *Information Systems* 59 (2016), 15–47.
- [31] E. Chávez and G. Navarro. 2005. A compact space decomposition for effective metric indexing. *Pattern Recognition Letters*, 26, 9 (2005), 1363–1376.
- [32] E. Chávez, G. Navarro, R. A. Baeza-Yates, and J. L. Marroquín. 2001. Searching in metric spaces. *ACM Computer Survey*, 33, 3 (2001), 273–321.
- [33] L. Chen, Y. Gao, X. Li, C. S. Jensen, and G. Chen. 2015. Efficient Metric Indexing for Similarity Search. In *ICDE*, 591–602.
- [34] L. Chen, Y. Gao, X. Li, C. S. Jensen, and G. Chen. 2017. Efficient metric indexing for similarity search and similarity joins. *IEEE Transactions on Knowledge and Data Engineering* 29, 3 (2017), 556–571.
- [35] L. Chen, Y. Gao, X. Li, C. S. Jensen, and B. Zheng. 2015. Indexing metric uncertain data for range queries. In *SIGMOD*, 951–965.
- [36] L. Chen, Y. Gao, X. Li, C. S. Jensen, and B. Zheng. 2017. Indexing metric uncertain data for range queries and range joins. *The VLDB Journal* 26, 4 (2017), 585–610.
- [37] L. Chen, Y. Gao, B. Zheng, C. S. Jensen, H. Yang, and K. Yang. 2017. Pivot-based Metric Indexing. *PVLDB* 10, 10 (2017), 1058–1069.
- [38] P. Ciaccia and M. Patella. 1998. Bulk loading the M-tree. In *Proceedings of the 9th Australian Conference (ADC)*, 15–26.
- [39] P. Ciaccia and M. Patella. 2000. The M<sup>2</sup>-tree: Processing Complex Multi-Feature Queries with Just One Index. In *DELOS workshop*.
- [40] P. Ciaccia and M. Patella. 2002. Searching in metric spaces with user-defined and approximate distances. *ACM Transactions on Database Systems* 27, 4 (2002), 398–437.
- [41] P. Ciaccia and M. Patella. 2017. The power of distance distributions: Cost models and scheduling policies for quality-controlled similarity queries. In *SISAP*, 3–16.
- [42] P. Ciaccia, M. Patella, and P. Zezula. 1997. M-tree: An efficient access method for similarity search in metric spaces. In *VLDB*, 426–435.
- [43] K. Clarkson. 2006. Nearest-neighbor searching and metric space dimensions. In *Nearest-Neighbor Methods for Learning and Vision: Theory and Practice*, 15–59.

- [44] R. Connor. 2016. Reference point hyperplane trees. In *SISAP*, 65–78.
- [45] R. Connor and A. Dearle. 2018. Querying metric spaces with bit operations. In *SISAP*, 33–46.
- [46] F. Dehne and H. Nolte-meier. 1987. Voronoi trees and clustering problems. *Information Systems* 12, 2 (1987), 171–175.
- [47] F. Dehne and H. Nolte-meier. 1988. Voronoi trees and clustering problems. In *Syntactic and Structural Pattern Recognition*, 185–194.
- [48] V. Dohnal. 2004. An access structure for similarity search in metric spaces. In *EDBT*, 133–143.
- [49] V. Dohnal, C. Gennaro, P. Savino, and P. Zezula. 2003. D-index: Distance searching index for metric data sets. *Multimedia Tools Applications*, 21, 1 (2003), 9–33.
- [50] V. Dohnal, C. Gennaro, and P. Zezula. 2003. Similarity join in metric spaces using eD-index. In *DEXA*, 484–493.
- [51] K. Figueroa, E. Chávez, G. Navarro, R. Paredes. 2006. On the least cost for proximity searching in metric spaces. In: *WEA*, 279–290.
- [52] K. Figueroa, E. Chávez, G. Navarro, R. Paredes. 2009. Speeding up spatial approximation search in metric spaces. *Journal of Experimental Algorithmics* 14 (2009), article 6.
- [53] K. Figueroa and N. Reyes. 2019. Permutation’s signatures for proximity searching in metric spaces. In *SISAP*, 151–159.
- [54] O. U. Florez and S. Lim. 2008. HRG: A graph structure for fast similarity search in metric spaces. In *International Conference on Database and Expert Systems Applications*, 57–64.
- [55] M. Franzke, T. Emrich, A. Züfle and M. Renz. 2016. Indexing multi-metric data. In *ICDE*, 1122–1133.
- [56] K. Fredriksson. 2005. Exploiting distance coherence to speed up range queries in metric indexes. *Information Processing Letters* 95, 1 (2005), 287–292.
- [57] K. Fredriksson. 2007. Engineering efficient metric indexes. *Pattern Recognition Letters* 28, 1 (2007), 75–84.
- [58] A. W.-C. Fu, P. M.-S. Chan, Y.-L. Cheung, Y. S. Moon. 2000. Dynamic vp-tree indexing for  $n$ -nearest neighbor search given pair-wise distances. *The VLDB Journal* 9, 2 (2000), 154–173.
- [59] J. Goldstein and R. Ramakrishnan, 2000. Contrast plots and p-sphere trees: Space vs. time in nearest neighbour searches. In: *VLDB*, 429–440.
- [60] M. L. Hetland. The basic principles of metric indexing. 2009. In *Swarm intelligence for multi-objective problems in data mining*, 199–232.
- [61] G. Hjaltason and H. Samet. 2003. Index-driven similarity search in metric spaces. *ACM Transactions on Database Systems* 28, 4 (2003), 17–580.
- [62] M. E. Houle, and M. Nett. Rank cover trees for nearest neighbor search. In *SISAP*, 16–29, 2013.
- [63] M. Ishikawa, H. Chen, K. Furuse, J. X. Yu, and N. Ohbo. 2000. MB<sup>+</sup>Tree: A dynamically updatable metric index for similarity search. In: *WAIM*, 356–373.
- [64] H. V. Jagadish, B. C. Ooi, K. L. Tan, C. Yu, and R. Zhang. 2005. iDistance: An adaptive B<sup>+</sup>-tree based indexing method for nearest neighbor search. *ACM Transactions on Database Systems* 30, 2 (2005), 364–397.
- [65] S. Jin, O. Kim, and W. Feng. 2013. M<sup>X</sup>-tree: A Double Hierarchical Metric Index with Overlap Reduction. In *International Conference on Computational Science and Its Applications*, 574–589.
- [66] C. T. Jr., R. F. S. Filho, A. J. M. Traina, M. R. Vieira, and C. Faloutsos. 2007. The omni-family of all-purpose access methods: A simple and effective way to make similarity search more efficient. *The VLDB Journal* 16, 4 (2007), 483–505.
- [67] C. T. Jr., A. Traina, R. F. S. Filho, and C. Faloutsos. 2002. How to improve the pruning ability of dynamic metric access methods. In *Proceedings of the 11th International Conference on Information and Knowledge Management*, 219–226.
- [68] C. T. Jr., A. Traina, B. Seeger, and C. Faloutsos. 2000. Slim-trees: High performance metric trees minimizing overlap between nodes. In *ICDE*, 51–65
- [69] I. Kalantari and G. McDonald. 1983. A data structure and an algorithm for the nearest point problem. *IEEE Transactions on Software Engineering* 9, 5 (1983), 631–634.
- [70] Z. Kouahla. 2011. Exploring Intersection Trees for Indexing Metric Spaces. In *CIIA*.
- [71] K. I. Lin, H. V. Jagadish, C. Faloutsos. 1994. The TV-tree: An index structure for high-dimensional data. *The VLDB Journal* 3, 4 (1994), 517–542.
- [72] B. Liu, Z. Wang, X. Yang, W. Wang, and B. L. Shi. 2006. A bottom-up distance-based index tree for metric space. In *RSKT*, 442–449.
- [73] J. Lokoč, J. Moško, P. Čech, and T. Skopal. 2014. On indexing metric spaces using cut-regions. *Information Systems*, 43 (2014), 1–19.
- [74] Y. Malkov, A. Ponomarenko, A. Logvinov, and V. Krylov. 2014. Approximate nearest neighbor algorithm based on navigable small world graphs. *Information Systems*, 45 (2014), 61–468.
- [75] R. Mao, W. L. Miranker, and D. P. Miranker. 2012. Pivot selection: Dimension reduction for distance-based indexing. *Journal of Discrete Algorithms* 13 (2012), 32–46.
- [76] M. Marin, R. Uribe, and R. Barrientos. 2007. Searching and updating metric space databases using the parallel egnat. In *International Conference on Computational Science*, 229–236.
- [77] J. Martinez and Z. Kouahla. 2012. Indexing metric spaces with nested forests. In *DEXA*, 458–465.

- [78] V. Mic, D. Novak, and P. Zezula. 2017. Sketches with unbalanced bits for similarity search. In *SISAP*, 53–63.
- [79] L. Mico and J. Oncina. 1994. A new version of the nearest-neighbour approximating and eliminating search algorithm (AESA) with linear preprocessing time and memory requirements. *Pattern Recognition Letters* 15, 1 (1994), 9–17.
- [80] L. Mico, J. Oncina, and R. C. Carrasco. 1996. A fast branch & bound nearest neighbour classifier in metric spaces. *Pattern Recognition Letters*, 17, 7 (1996), 731–739.
- [81] H. Mohamed and S. Marchand-Maillet. 2015. Quantized ranking for permutation-based indexing. *Information Systems*, 52 (2015), 163–175.
- [82] J. Mosko, J. Lokoc, and T. Skopal. 2011. Clustered pivot tables for I/O-optimized similarity search. In *SISAP*, 17–24.
- [83] B. Naidan, L. Boytsov, and E. Nyberg. 2015. Permutation search methods are efficient, yet faster search is possible. *PVLDB* 8, 12 (2015), 1618–1629.
- [84] G. Navarro. 1999. Searching in metric spaces by spatial approximation. In *Proceedings of the 6th International Symposium on String Processing and Information Retrieval*, 141–148.
- [85] G. Navarro. 2002. Searching in metric spaces by spatial approximation. *The VLDB Journal*, 11, 1 (2002), 8–46.
- [86] G. Navarro and N. Reyes. 2001. Dynamic spatial approximation trees. In *Proceedings of the XXI Conference of the Chilean Computer Science Society (SCCC)*, 213–222.
- [87] G. Navarro and N. Reyes. 2002. Fully dynamic spatial approximation trees. In *Proceedings of the 9th International Symposium on String Processing and Information Retrieval*, 254–270.
- [88] G. Navarro and N. Reyes. 2003. Improved deletions in dynamic spatial approximation trees. In *Proceedings of the XXIII International Conference of the Chilean Computer Science Society (SCCC)*, article 13.
- [89] G. Navarro and R. U. Paredes. 2011. Fully dynamic metric access methods based on hyperplane partitioning. *Information Systems* 36, 4 (2011), 734–747.
- [90] G. Navarro and N. Reyes. 2009. Dynamic spatial approximation trees for massive data. In *SISAP*, 81–88.
- [91] G. Navarro and N. Reyes. 2016. New dynamic metric indices for secondary memory. *Information Systems*, 59 (2016), 48–78.
- [92] H. Noltemeier, K. Verbarg, and C. Zirkelbach. 1992. Monotonous bisector\* Trees – A tool for efficient partitioning of complex scenes of geometric objects. In *Data Structure and Efficient Algorithms*, 186–203.
- [93] D. Novak, M. Batko, and P. Zezula. 2011. Metric Index: An efficient and scalable solution for precise and approximate similarity search. *Information Systems* 36, 4 (2011), 721–733.
- [94] D. Novak and P. Zezula. 2016. PPP-codes for large-scale similarity searching. In *Transactions on Large-Scale Data- and Knowledge-Centered Systems XXIV*, 61–87.
- [95] A. Ocsa, C. Bedregal, and E. Cuadros-Vargas. 2007. A new approach for similarity queries using neighborhood graphs. In *Brazilian Symposium on Databases*, 131–142.
- [96] R. Paredes and E. Chavez. 2005. Using the  $k$ -nearest neighbor graph for proximity searching in metric spaces. In *SPIRE*, 127–138.
- [97] V. Pestov. 2012. Indexability, concentration, and VC theory. *Journal of Discrete Algorithms* 13 (2012), 2–18.
- [98] I. R. V. Pola, C. Traina Jr, and A. J. M. Traina. 2007. The MM-tree: A memory-based metric tree without overlap between nodes. In *ADBI*, 157–171.
- [99] D. A. Rachkovskij. 2017. Distance-based index structures for fast similarity search. *Cybernetics and Systems Analysis* 53, 4 (2017), 636–658.
- [100] H. Razente and M. C. N. Barioni. 2019. Storing data once in M-tree and PM-tree. In *SISAP*, 18–31.
- [101] H. Razente, R. M. S. Sousa, and M. C. N. Barioni. 2018. Metric indexing assisted by short-term Memories. In *SISAP*, 107–121.
- [102] E. V. Ruiz. 1986. An algorithm for finding nearest neighbours in (approximately) constant average time. *Pattern Recognition Letters* 4, 3 (1986), 145–157.
- [103] G. Ruiz, F. Santoyo, E. Chávez, K. Figueroa, and E. S. Tellez. 2013. Extreme pivots for faster metric indexes. In *SISAP*, 115–126.
- [104] K. Al Ruqeishi and M. Konečný. 2015. Regrouping metric-space search index for search engine size adaptation. In *SISAP*, 271–282.
- [105] U. Shaft and R. Ramakrishnan. 2006. Theory of nearest neighbors indexability. *ACM Transactions on Database Systems*, 31 (2006), 814–838.
- [106] L. C. Shimomura and D. S. Kaster. 2019. HGraph: A connected-partition approach to proximity graphs for similarity search. In *International Conference on Database and Expert Systems Applications*, 106–121.
- [107] L. C. Shimomura, M. R. Vieira, and D. S. Kaster. 2018. Performance analysis of graph-based methods for exact and approximate similarity search in metric spaces. In *SISAP*, 18–32.
- [108] T. Skopal and D. Hoksza. 2007. Improving the performance of M-tree family by nearest neighbor graphs. In: *ADBI*, 172–188.
- [109] T. Skopal and J. Lokoč. 2008. NM-tree: Flexible approximate similarity search in metric and non-metric spaces. In *DEXA*, 312–325.

- [110] T. Skopal and J. Lokoč. 2009. New dynamic construction techniques for M-tree. *Journal of Discrete Algorithms* 7, 1 (2009), 62–77.
- [111] T. Skopal, J. Pokorný, M. Kratky, and V. Snasel. 2003. Revisiting M-tree building principles. In *ADBIS*, 148–162.
- [112] T. Skopal, J. Pokorný, and V. Snasel. 2004. PM-tree: Pivoting metric tree for similarity search in multimedia databases. In *ADBIS*, 803–815.
- [113] K. Tokoro, K. Yamaguchi, and S. Masuda. 2006. Improvements of TLAESA nearest neighbor search algorithm and extension to approximation search. In *Proceedings of the 29th Australasian Computer Science Conference*, 77–83.
- [114] J. K. Uhlmann. 1991. Metric trees. *Applied Mathematics Letters* 4, 5 (1991), 61–62.
- [115] J. K. Uhlmann. 1991. Satisfying general proximity/similarity queries with metric trees. *Information Processing Letters*, 40, 4 (1991), 175–179.
- [116] L. Vadicamo, R. Connor, F. Falchi, C. Gennaro, and F. Rabitti. 2019. SPLX-Perm: A novel permutation-based representation for approximate metric search. In *SISAP*, 40–48.
- [117] E. Vidal. 1986. An algorithm for finding nearest neighbors in (approximately) constant average time. *Pattern Recognition Letters* 4, 3 (1986), 145–157.
- [118] J. M. Vilar. 1995. Reducing the overhead of the AESA metric-space nearest neighbor searching algorithm. *Information Processing Letters* 56, 5 (1995), 265–271.
- [119] M. R. Vieira, C. T. Jr, F. J. T. Chino, and A. J. M. Traina. 2004. DBM-tree: A dynamic metric access method sensitive to local density data. In *SBBD*, 163–177.
- [120] M. R. Vieira, C. T. Jr, F. J. T. Chino, and A. J. M. Traina. 2010. DBM-tree: A dynamic metric access method sensitive to local density data. *Journal Information and Data Management* 1, 1 (2010) 111–127.
- [121] I. Volnyansky and V. Pestov. 2009. Curse of dimensionality in pivot based indices. In *SISAP*, 39–46.
- [122] P. N. Yianilos. 1993. Data structures and algorithms for nearest neighbor search in general metric spaces. In *SODA*, 311–321.
- [123] P. N. Yianilos. 1999. Excluded middle vantage point forests for nearest neighbor search. *Technical report, NEC Research Institute*.
- [124] P. Zezula, G. Amato, V. Dohnal, and M. Batko. 2006. Similarity search: The metric space approach. *Springer Science & Business Media*.
- [125] P. Zezula, P. Savino, G. Amato, and F. Rabitti. 1998. Approximate Similarity Retrieval with M-Trees. *The VLDB Journal* 4 (1998), 275–293.
- [126] M. Zhang and R. Alhajj. 2010. Effectiveness of NAQ-tree as index structure for similarity search in high-dimensional metric space. *Knowledge and information systems* 22, 1 (2010), 1–26.
- [127] X. Zhou, G. Wang, J. X. Yu, G. Yu. 2003. M<sup>+</sup>-tree: A new dynamical multidimensional index for metric spaces. In *ADC*, 161–168.
- [128] X. Zhou, G. Wang, X. Zhou, and G. Yu. 2005. BM<sup>+</sup>-tree: A hyperplane-based index method for high-dimensional metric spaces. In *International Conference on Database Systems for Advanced Applications*, 398–409.